Supporting Information

Post-synthetic modification of amine-functionalized permanently porous coordination cages

Jahidul Hoq,[a] Michael R. Dworzak,[b] Duleeka Dissanayake,[a] Rebecca X. Skalla,[a] Nobuyuki Yamamoto,[a] Glenn P. A. Yap[b] and Eric D. Bloch*[a]

[a]Department of Chemistry, Indiana University, Bloomington, Indiana 47405, United States

[b]Department of Chemistry & Biochemistry, University of Delaware, Newark, Delaware 19716, United States

List of Contents

Experimental Details	S3-5
Gas Adsorption Isotherms and Studies	S7-9
NMR Spectra	S10-28
UV-vis Absorption	S28-32
XPS	S33
IR	S34-36
MS	S37
References	S41

Materials and Methods. Unless otherwise noted, reagents and solvents were sourced commercially and used without further purification. Porous cages were synthesized and modified in an N_2 glovebox using airfree solvents that were dispensed from a solvent purification system and stored over appropriately sized sieves prior to use. Aldehydes precursors and NMR solvents were degassed via three freeze-pump-thaw cycles and brought into a glovebox and stored over sieves for 3 days before use. Acid digestions of the cages were performed by adding one drop of 35 wt.% DCl in D_2O and 0.5 mL of DMSO-d_6 to a 4 mL vial containing approximately 10 mg of cage, then sonicated until a homogeneous solution is obtained. UV-vis samples were prepared in the glove box by dissolving cages in air free dry solvents, and spectra were recorded in a closed cuvette avoiding any air exposure.

Low-pressure gas adsorption measurements were performed using a Micromeritics Tristar 3000 at 195 K. After exchanging DEF, THF, and DCM, the solvent was decanted, and the residual solvents were removed to obtain the cage materials. Samples were activated under dynamic vacuum at an optimal temperature for each material using a Micromeritics smart vac prep. Infrared (IR) spectra were recorded with a Bruker α II instrument equipped with a diffuse reflectance ATR attachment. Ultraviolet-visible (UV-vis) spectra were measured using a JASCO V-750(ST) spectrometer, a deuterium-halogen source attached, while a JASCO ISV-9222-60 nm Integrating Sphere was used for diffuse reflectance measurement. Elemental analyses were conducted using a PHI VersaProbe II Scanning X-ray Microprobe photoelectron spectroscopy (XPS) at the Indiana University Bloomington's Surface Analysis Facility.

^{1}H NMR, ^{19}F NMR, and ^{31}P spectra were obtained using a Bruker AV 400 MHz spectrometer, and the data were processed using MestReNova NMR software.

Synthesis of Mo_{24}(5-NH_2-bdc)$_{24}$: In a 20 mL vial, molybdenum acetate (0.10 g, 0.23 mmol) and 5-NH_2-bdc (0.038 g, 0.23 mmol) were dissolved in 10 mL of dry DEF. The solution was heated at 120 °C for 48 hours, producing an orange-colored crystalline solid. Additional cages dissolved in DEF were precipitated by adding 10 mL of THF. The resulting cage was separated by centrifugation and washed with fresh THF three times, every 12 hours. The final dried samples were obtained by activating them under reduced pressure at room temperature overnight.

Synthesis of Mo_{24}(m-bdc)$_{24}$
Molybdenum acetate (0.10 g, 0.23 mmol) and isophthalic acid, m-bdc, (0.038 g, 0.23 mmol) were dissolved in 8 mL of dry DMF in a 20 ml vial. 2 ml of MeOH was added to the solution and heated at 100 °C for 2 days. 5 ml of diethyl ether solvent was added to the cooled down solution to precipitate the dissolved cage and washed with same solvent for three times every 12 hours. The final washed cage was vacuum dried at RT and activated at 75 °C.

Synthesis of [Zr_{12}(μ_3-O)$_4$(μ_2-OH)$_{12}$(Cp)$_{12}$(2-NH_2-bdc)$_6$]Cl_4: In a 20 ml vial, $ZrCp_2Cl_2$ (0.175 g, 0.59 mmol) and 2-NH_2-bdc (0.095 g, 0.52 mmol) were dissolved in 10 ml DEF

and 500 μl H_2O. The solution was then heated at 65 °C for 12 hours, resulting in yellow crystalline cage material. The cage material was then centrifuged and separated upon removal of DEF. The separated cage was then washed with DEF and $CHCl_3$ three times each for 12 hours. The final activated sample was obtained by drying at RT under a dynamic vacuum.

Synthesis of $[(Mg_4SC4A)_4(\mu_4\text{-}OH)_4(5\text{-}NH_2\text{-}bdc)_8]$: $MgCl_2$ (100 mg. 0.33 mmol), sulfonylcalix[4]arenes (SC4A) (85 mg, 0.33 mmol) was dissolved in 6 ml DMF and 4 ml MeOH in a 20 ml vial and heated up at 85 °C for 12 hours. 5-NH_2-bdc (0.59 g, 0.33 mmol) was added to the warmed solution and light crystalline cage was formed upon heating at 85 °C for another 12 hours. The cage was then washed with MeOH three times every 12 hours and the final cage was activated at 100 °C under vacuum conditions.

2-formylpyridine functionalization of $[Zr_{12}(\mu_3\text{-}O)_4(\mu_2\text{-}OH)_{12}(Cp)_{12}(2\text{-}NH_2\text{-}bdc)_6]Cl_4$: In a 20 ml vial, activated $[Zr_{12}(\mu_3\text{-}O)_4(\mu_2\text{-}OH)_{12}(Cp)_{12}(2\text{-}NH_2\text{-}bdc)_6]Cl_4$ (0.067 g, 0.02 mmol) was suspended in 10 ml THF upon addition of 2-formylpyridine (0.05 mmol). The mixture was then stirred for 4 days at RT and imine functionalized cage was separated from THF upon centrifugation. Another 5 THF wash was performed to remove excess 2-formylpyridine and then activated at 50 °C under dynamic vacuum.

2-formylpyridine functionalization of $[(Mg_4SC4A)_4(\mu_4\text{-}OH)_4(5\text{-}NH_2\text{-}bdc)_8$: Activated $[(Mg_4SC4A)_4(\mu_4\text{-}OH)_4(5\text{-}NH_2\text{-}bdc)_8$ (0.056 g, 0.01 mmol) was suspended in 10 ml THF in a 20 ml vial and 0.05 mmol 2-formylpyridine was added to the vial. The cage mixture was then stirred for 4 days at RT and washed with fresh THF five times upon centrifugation. The imine cage was then vacuum dried at 100 °C for 2 days.

Imine functionalization of $Mo_{24}(5\text{-}NH_2\text{-}bdc)_{24}$: Activated $Mo_{24}(5\text{-}NH_2\text{-}bdc)_{24}$ (0.065 g, 0.01 mmol) was placed in a 20 mL vial, followed by the addition of a 0.05 mmol of each aldehyde, 2-formylpyridine, 3-formylpyridine, 4-formylpyridine, benzaldehyde and hexanal. Then, the mixture was stirred for 2 days upon addition of 10 ml THF. The resulting functionalized cages were separated by centrifugation and the supernatant was decanted. Excess aldehydes were removed by washing with DCM five times, every 12 hours. The final cages were obtained by activating them at 75 °C under dynamic vacuum.

Metallation to Mo_{24}(2-pyridineimine-bdc)$_{24}$: Mo_{24}(2-pyridineimine-bdc)$_{24}$ (0.0876 g, 0.01 mmol) was placed in a 20 mL vial, and 5 mL dry THF solutions of [(S)-(-)2,2'-Bis(diphenylphosphino)-1,1'-binaphthyl]-diaquo-palladium(II) bis (triflate); $Pd(OTf)_2$ (0.2544 g, 0.24 mmol) and $CoCl_2$ (0.0309 g, 0.24 mmol) were prepared separately for Pd and Co metalation. The respective $Pd(OTf)_2$ and $CoCl_2$ solutions were added to the vial and stirred for 2 days. The metallated cage was then separated and vacuum-activated at room temperature after being washed with dry THF three times.

Synthesis of dimethyl-2-pyridineimine-bdc ligand: dimethyl-5-NH_2-bdc **(**2.09 g, 10.0 mmol) and 0.01 mol 2-formylpyridine was added to a 250 ml RBF and 50 ml of anhydrous $CHCl_3$ was cannula transferred into it followed by stirring at RT for 2 days. $CHCl_3$ soluble dimethyl-2-pyridineimine-bdc was separated and dried under reduced pressure. Excess

dimethyl-5-NH_2-bdc and 2-formylpyridine was removed by washing with water for 5 times and pure dimethyl-2-pyridineimine-bdc was dried at 120 °C in an oven.

Co and Pd metalation to dimethyl-2-pyridineimine-bdc: $CoCl_2$ (0.025 g, 0.2 mmol) was dissolved in 5 ml acetonitrile in a 20 ml vial along with a separate solution of dimethyl-2-pyridineimine-bdc (0.0596 g, 0.2 mmol) in 5 ml acetonitrile. Both solutions were added together and heated at 70 °C for 12 hours resulting in blue-green color $CoCl_2$_dimethyl-2-pyridineimine-bdc solution. Diffraction-quality single crystals were obtained by Benzene diffusion into the solution.

Equimolar solutions of $Pd(CH_3CN)_2Cl_2$ (0.052 g, 0.2 mmol) and dimethyl-2-pyridineimine-bdc (0.0596 g, 0.2 mmol) were prepared in 10 ml acetonitrile and heated at 70 °C overnight, resulting in golden $PdCl_2$_dimethyl-2-pyridineimine-bdc crystals.

An identical solution was prepared for $Pd(OTf)_2$ (0.0212 g, 0.02 mmol) and dimethyl-2-pyridineimine-bdc (0.02 mmol) in 10 ml THF and allowed to react at RT overnight, generating highly soluble $Pd(OTf)_2$_dimethyl-2-pyridineimine-bdc. The metallated bdc was precipitated out by adding hexane and dried at RT.

Imine formation kinetic study of dimethyl-5-NH_2-bdc: 0.05 mmol of each aldehyde was added to 0.01 mmol of dimethyl-5-NH_2-bdc ligand in anhydrous THF. A 0.5 mL portion of the solution was transferred into NMR tubes via cannula transfer, and ^{1}H-NMR spectra were recorded after 2, 4, 20, and 38 hours.

Benzaldehyde treatment to Mo_{24}(m-bdc)$_{24}$

Mo_{24}(m-bdc)$_{24}$ (0.062 g, 0.01 mmol) and 0.05 mmol of benzaldehyde were suspended into 10 ml of THF in a 20 ml vial. The mixture was then stirred for 2 days and suspended cage was separated by centrifugation. Excess aldehydes were removed by washing with DCM five times, every 12 hours. The final cages were obtained by activating them at 75 °C under dynamic vacuum.

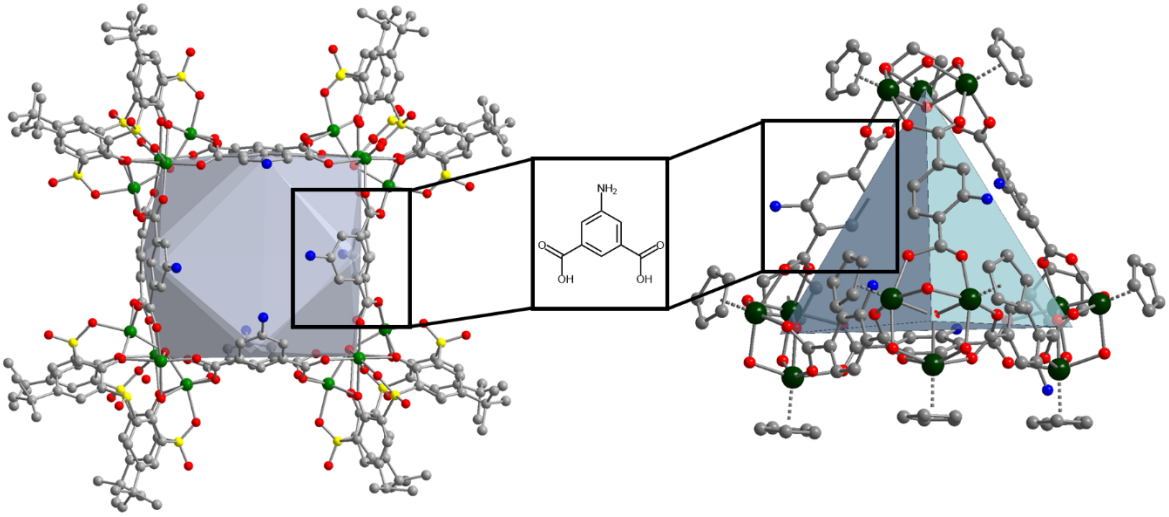

$[(Mg_4SC4A)_4(\mu 4\text{-}OH)_4(5\text{-}NH_2\text{-}bdc)_8]^{4-}$ $[Zr_{12}(\mu_3\text{-}O)_4(\mu_2\text{-}OH)_{12}(Cp)_{12}(2\text{-}NH_2\text{-}bdc)_6]^{4+}$

Figure S1. Structure of cuboctahedron $[(Mg_4SC4A)_4(\mu_4\text{-}OH)_4(5\text{-}NH_2\text{-}bdc)_8]^{4-}$ and tetrahedron $Zr_{12}(\mu_3\text{-}O)_4(\mu_2\text{-}OH)_{12}(Cp)_{12}(2\text{-}NH_2\text{-}bdc)_6]^{4+}$ cage containing 5-NH_2-bdc and 2-NH_2-bdc ligands respectively.

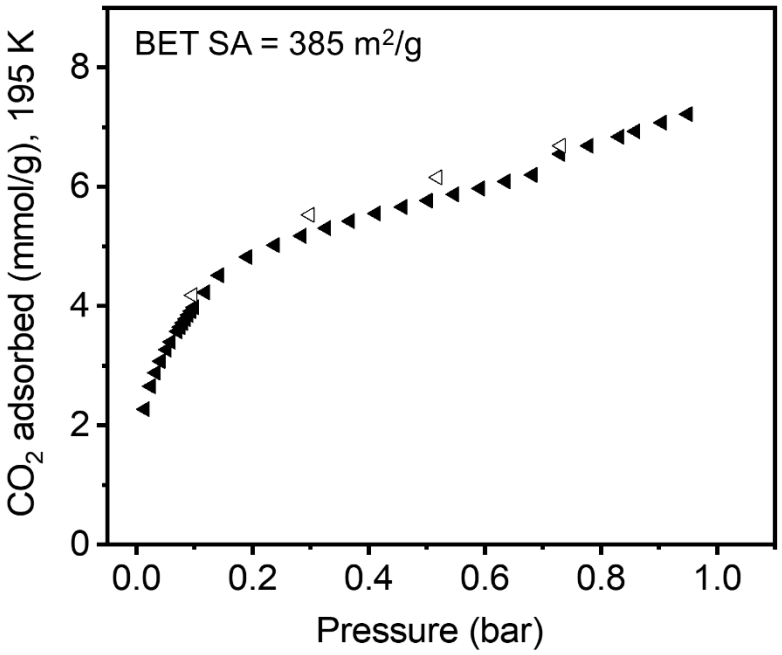

Figure S2. Full CO_2 BET isotherm of $Zr_{12}(\mu_3\text{-}O)_4(\mu_2\text{-}OH)_{12}(Cp)_{12}(2\text{-}NH_2\text{-}bdc)_6]Cl_4$ cage activated at 50 °C.

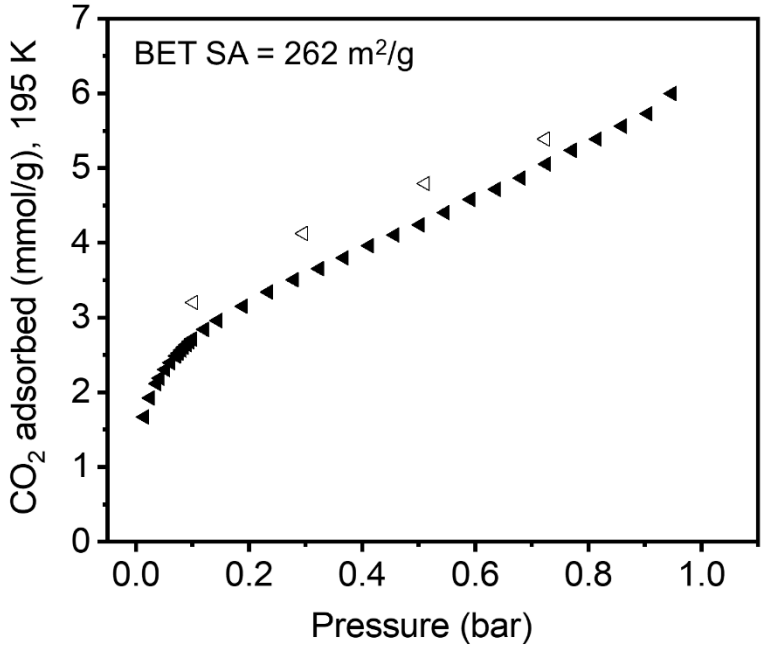

Figure S3. Full CO_2 BET isotherm of $[(Mg_4SC4A)_4(\mu_4\text{-}OH)_4(5\text{-}NH_2\text{-}bdc)_8]$ cage activated at 100 °C.

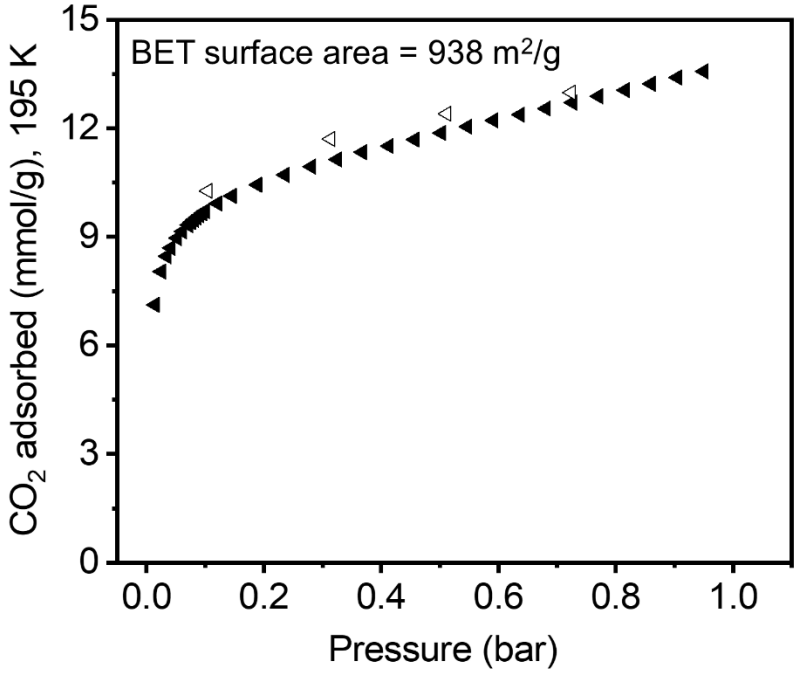

Figure S4. Full CO_2 BET isotherm of $Mo_{24}(5\text{-}NH_2\text{-}bdc)_{24}$ cage activated at 75 °C.

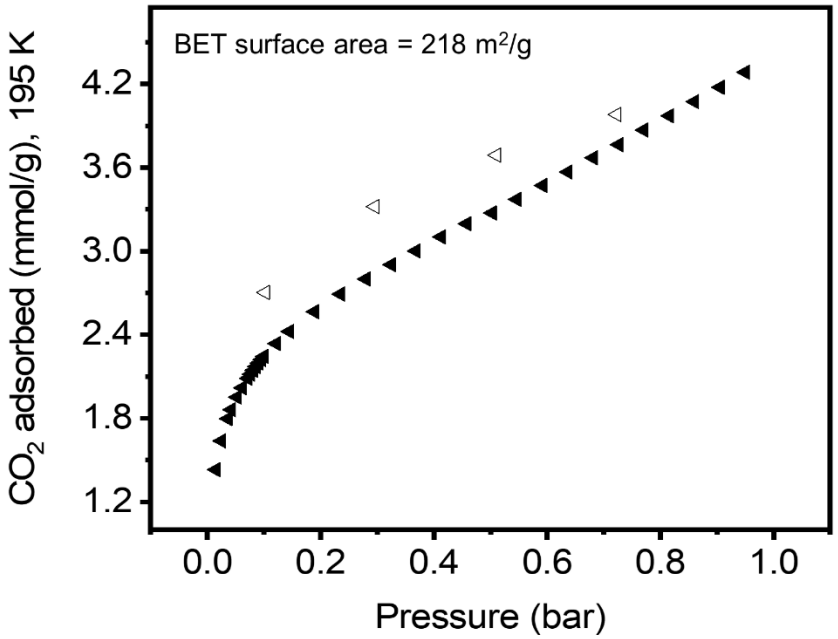

Figure S5. Full CO_2 BET isotherm of $Zr_{12}(\mu_3\text{-}O)_4(\mu_2\text{-}OH)_{12}(Cp)_{12}(2\text{-pyridineimine-bdc})_6]Cl_4$ cage activated at 75 °C.

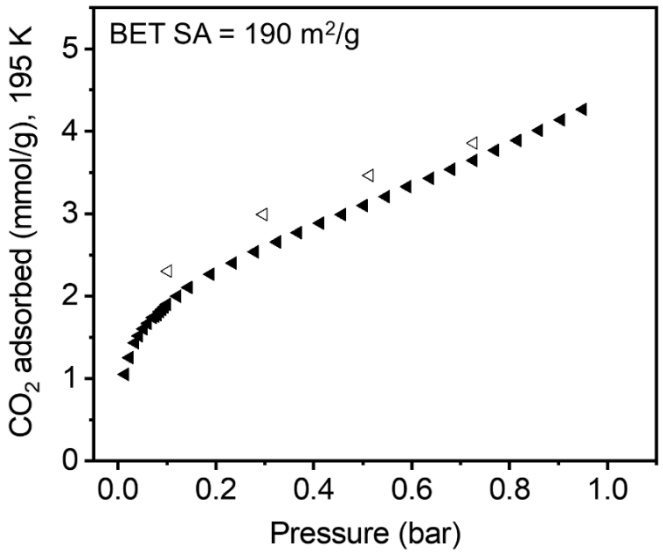

Figure S6. Full CO_2 BET isotherm of $[(Mg_4SC4A)_4(\mu_4\text{-}OH)_4(2\text{-pyridineimine-bdc})_8]$ cage activated at 100 °C.

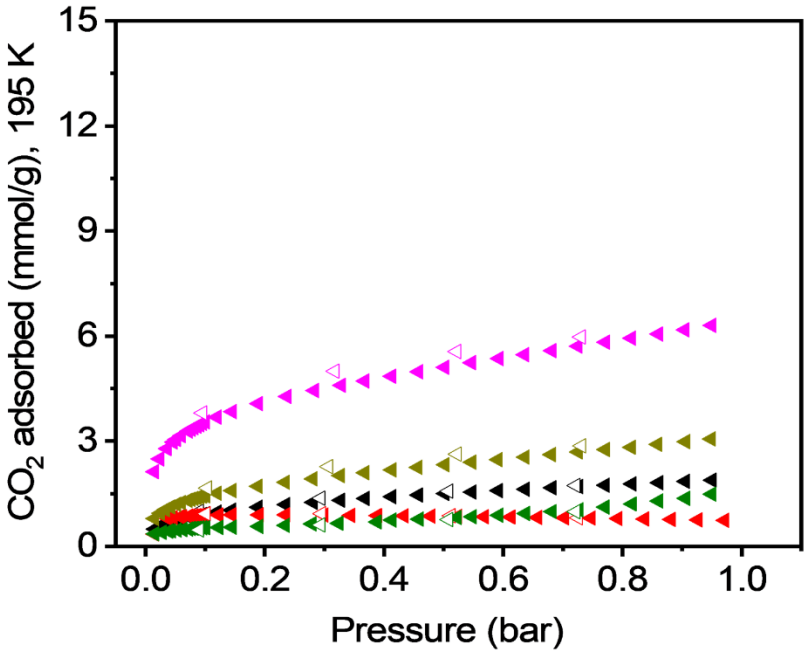

Figure S7. Full CO_2 BET isotherm of Mo_{24}(2-pyridineimine-bdc)$_{24}$, black; Mo_{24}(3-pyridineimine-bdc)$_{24}$, green; Mo_{24}(4-pyridineimine-bdc)$_{24}$, red; Mo_{24}(benzalimine-bdc)$_{24}$, pink; and Mo_{24}(hex-imine-bdc)$_{24}$, olive showing BET surface areas of 97, 94, 116, 356 and 144 m^2/g respectively for corresponding cages activated at 75 °C.

^{1}H-NMR Spectra

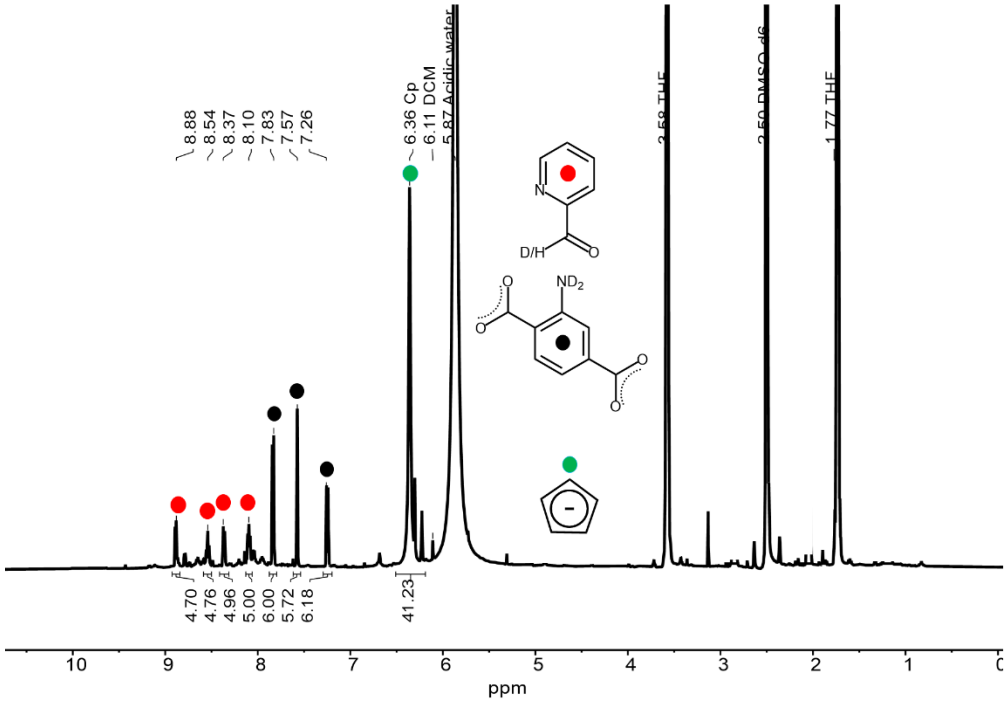

Figure S8. ^{1}H-NMR spectrum of DCl digested $Zr_{12}(\mu_3\text{-}O)_4(\mu_2\text{-}OH)_{12}(Cp)_{12}(2\text{-}NH_2\text{-}bdc)_6]Cl_4$. The spectrum was recorded in deuterated DMSO.

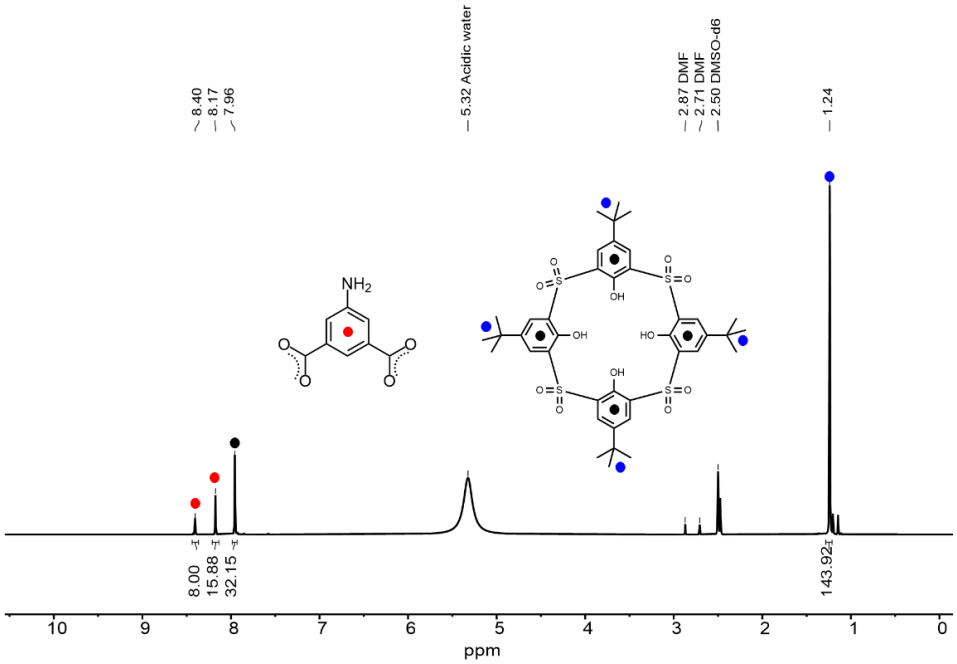

Figure S9. ^{1}H-NMR spectrum of DCl digested $[(Mg_4SC4A)_4(\mu_4\text{-}OH)_4(5\text{-}NH_2\text{-}bdc)_8]$. The spectrum was recorded in deuterated DMSO.

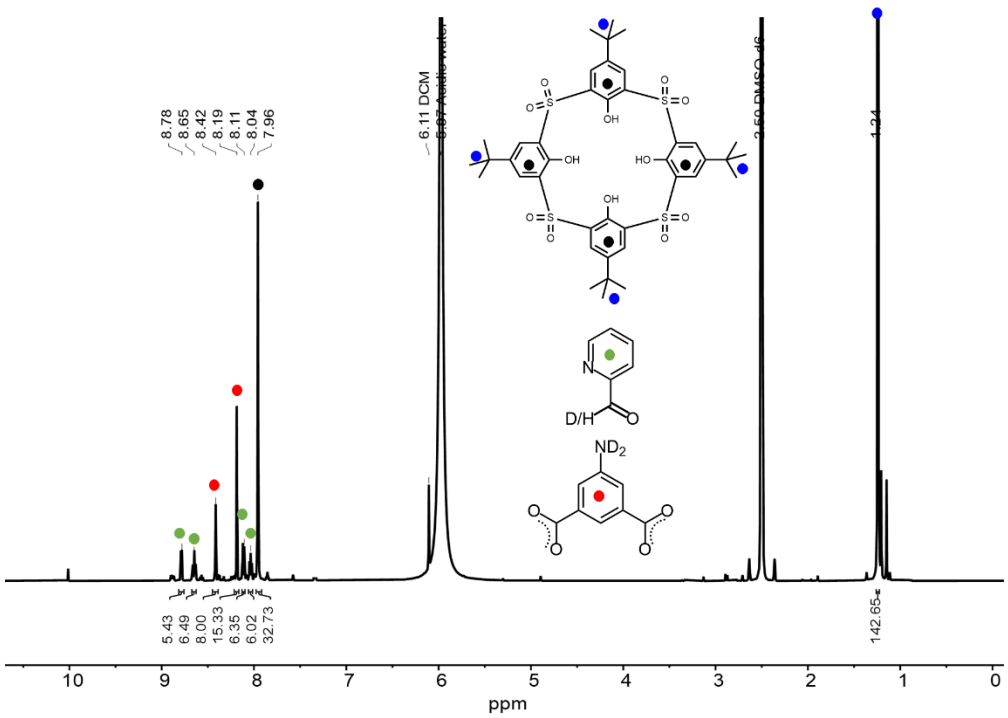

Figure S10. ^{1}H-NMR spectrum of DCl digested [$(Mg_4SC4A)_4(\mu_4\text{-}OH)_4$(2-pyridineimine-bdc)$_8$]. The spectrum was recorded in deuterated DMSO.

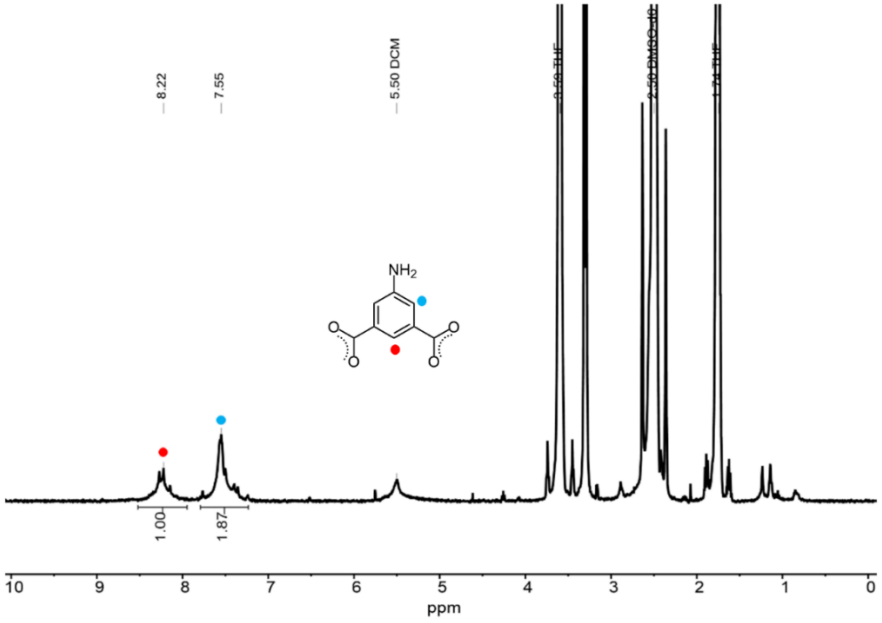

Figure S11. ^{1}H-NMR spectrum of Mo_{24}(5-NH_2-bdc)$_{24}$ in DMSO-d_6. Cage resonances are broad as a result of the size of the cage and the slight paramagnetism of the Mo-Mo unit.

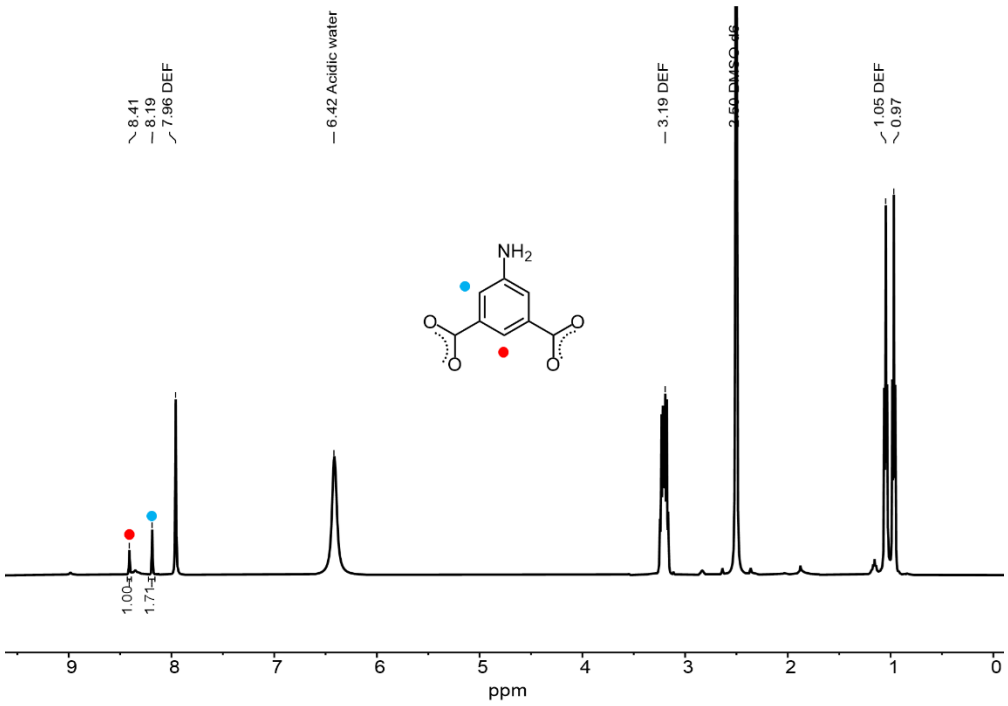

Figure S12. ^{1}H-NMR spectrum of DCl digested Mo_{24}(5-NH_2-bdc)$_{24}$ in DMSO-d_6.

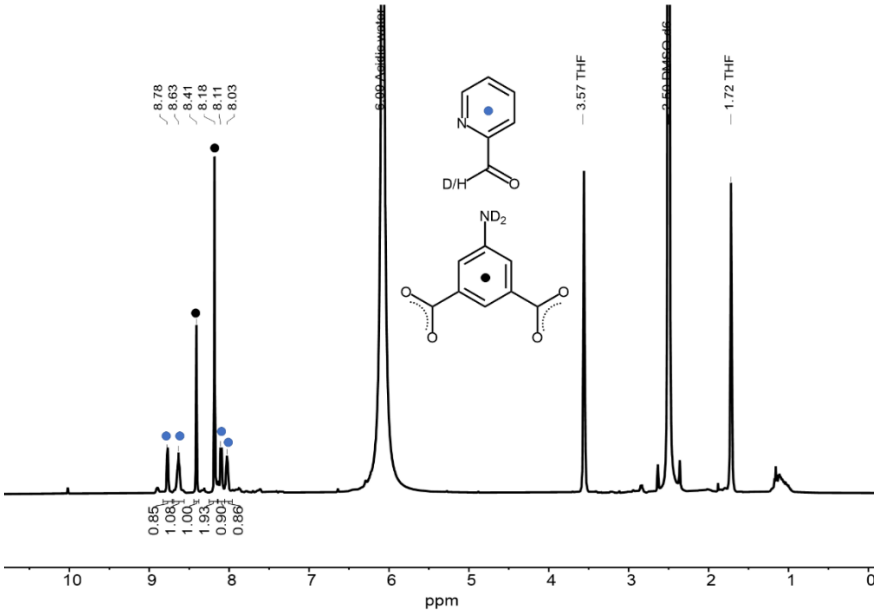

Figure S13. ^{1}H-NMR spectrum of DCl digested Mo_{24}(2-pyridineimine-bdc)$_{24}$ in DMSO-d_6. Hydrolysis of the imine under these conditions affords aldehyde where the aldehyde-proton is partially exchanged with deuterated solvent. The ratio of aldehyde to amine in hydrolyzed sample (~1:1) in conjunction with IR spectra of the imine-based material suggests stoichiometric imine in the starting material.

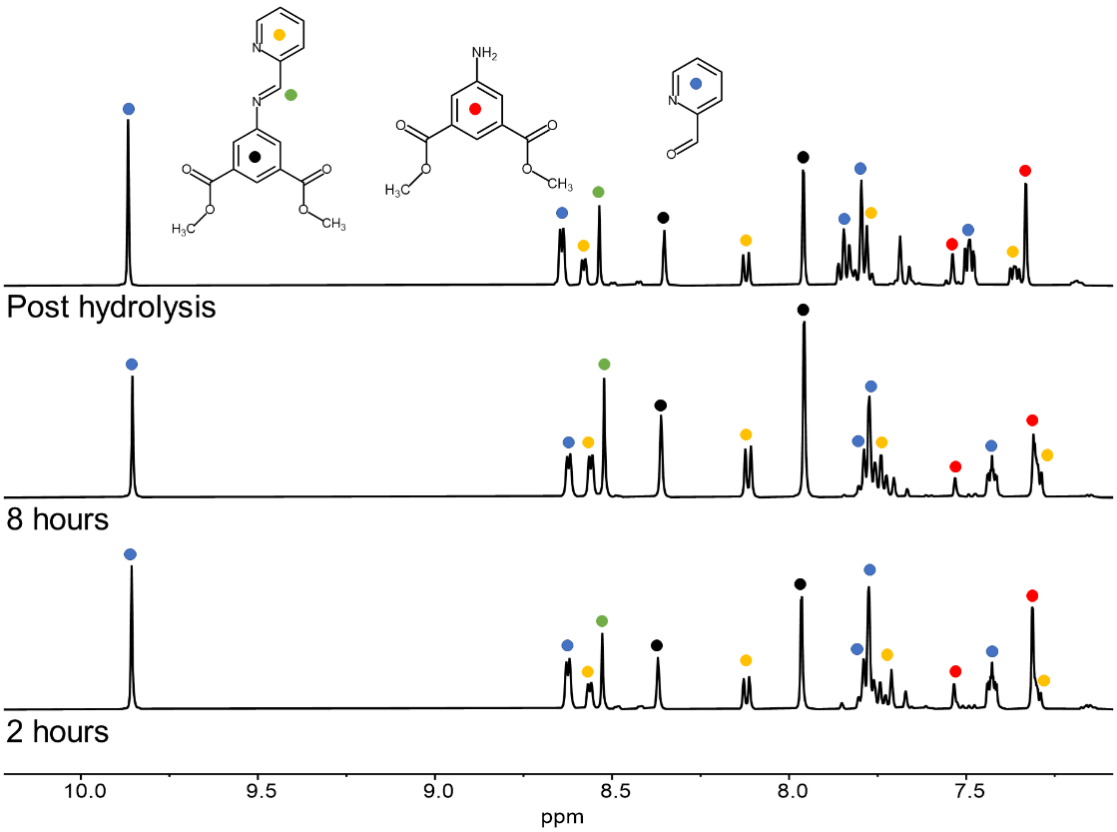

Time (hour)	Unreacted dimethyl-5-NH_2-bdc	Imine formed
2	1	1.51
8	1	2.34
Post hydrolysis	1	1.66

Figure S14. ^{1}H-NMR spectra of dimethyl-2-pyridineimine-bdc in DMSO-d_6. Imine formation was integrated compared to unreacted dimethyl-5-NH_2-bdc ligand.

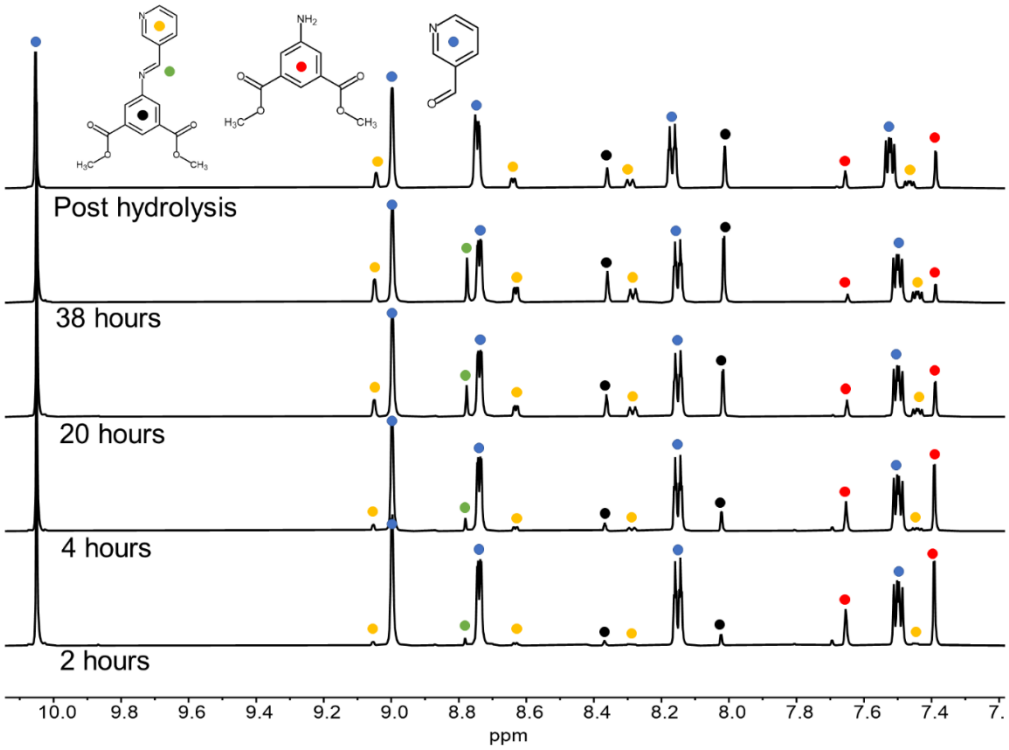

Time (hour)	Unreacted dimethyl-5-NH_2-bdc	Imine formed
2	1	0.12
4	1	0.24
20	1	0.58
38	1	0.78
Post hydrolysis	1	0.56

Figure S15. ^{1}H-NMR spectra of dimethyl-3-pyridineimine-bdc ligand in DMSO-d_6. Imine formation was integrated compared to unreacted dimethyl-5-NH_2-bdc ligand.

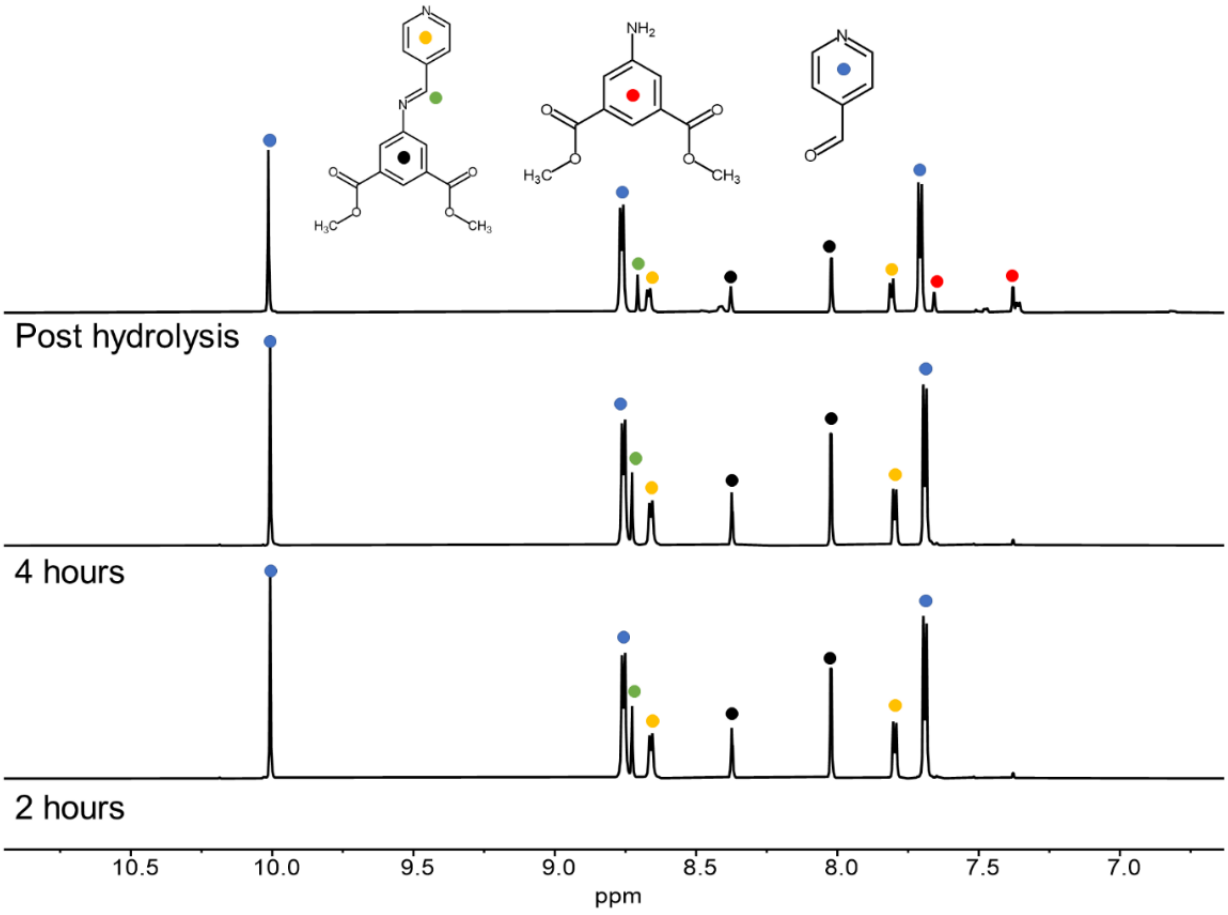

Time (hour)	Unreacted dimethyl-5-NH_2-bdc	Imine formed
2	1	5.74
4	1	5.89
Post hydrolysis	1	1.81

Figure S16. ^{1}H-NMR spectra of dimethyl-4-pyridineimine-bdc ligand in DMSO-d_6. Imine formation was integrated compared to unreacted dimethyl-5-NH_2-bdc ligand.

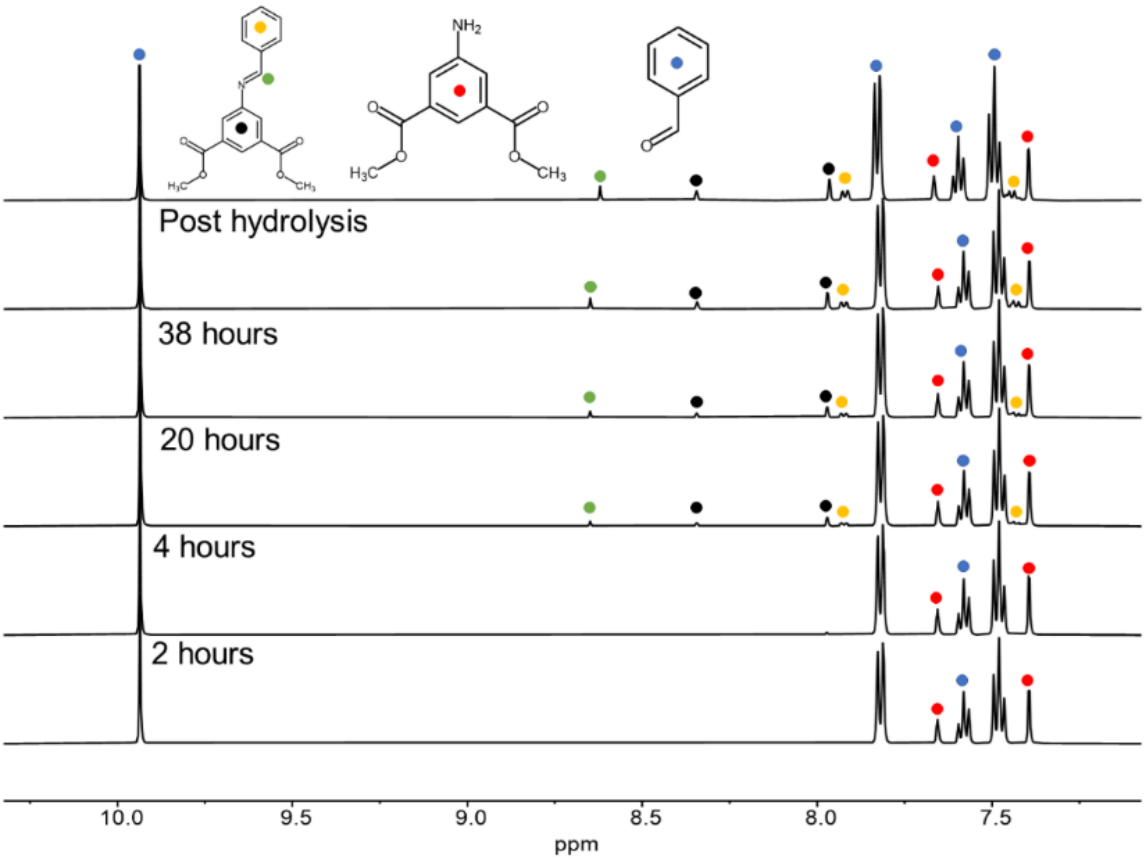

Time (hour)	Unreacted dimethyl-5-NH_2-bdc	Imine formed
2	1	0.029
4	1	0.0476
20	1	0.152
38	1	0.244
Post hydrolysis	1	0.229

Figure S17. ^{1}H-NMR spectra of dimethyl-benzalimine-bdc ligand in DMSO-d_6. Imine formation was integrated compared to unreacted dimethyl-5-NH_2-bdc ligand.

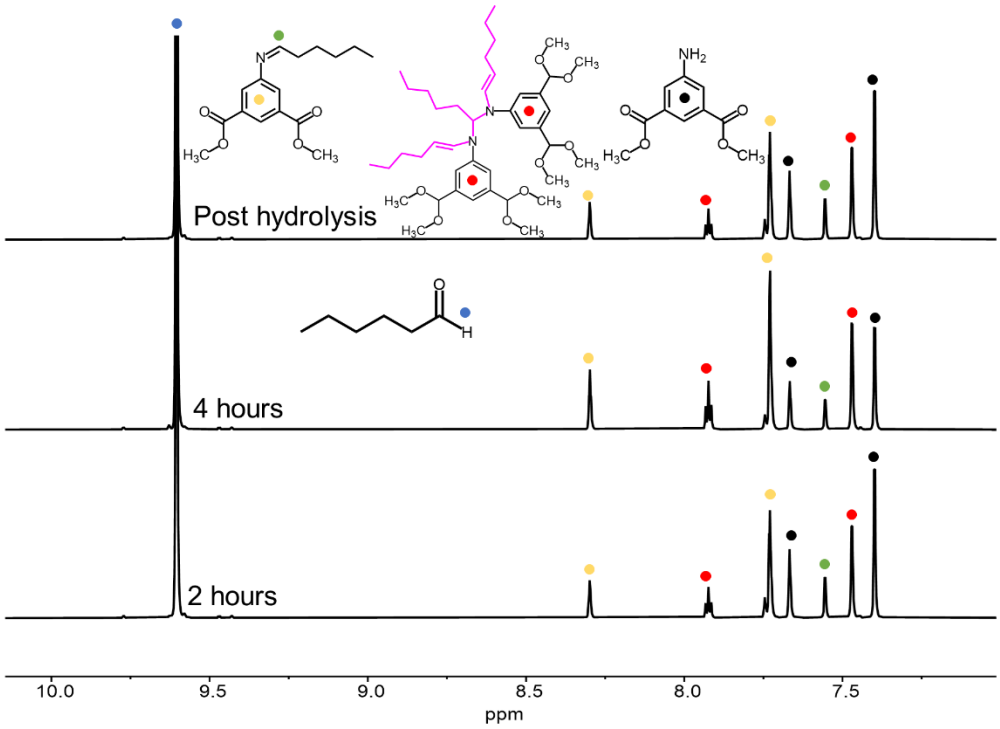

Time (hour)	Unreacted dimethyl-5-NH_2-bdc	Imine formed
2	1	1.74
4	1	2.39
Post hydrolysis	1	1.94

Figure S18. ^{1}H-NMR spectra of dimethyl-hex-imine-bdc in DMSO-d_6. Imine formation was integrated compared to unreacted dimethyl-5-NH_2-bdc ligand.

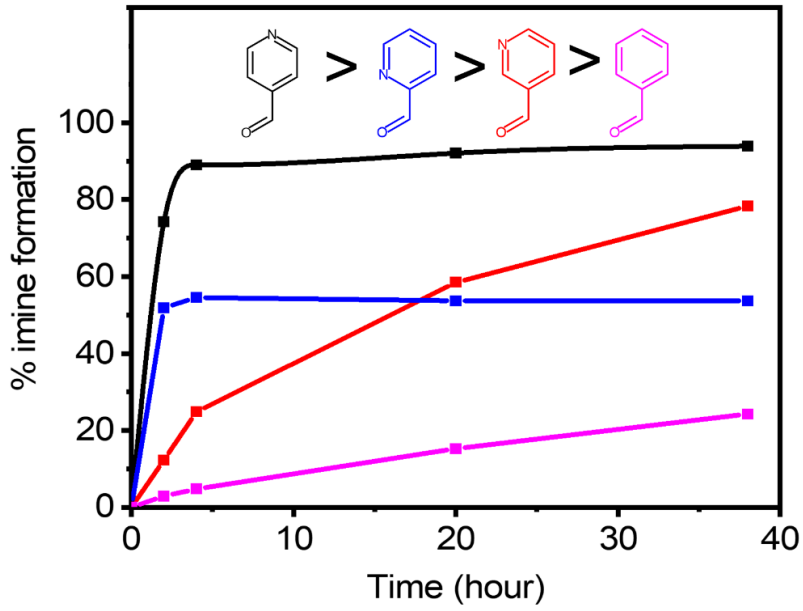

Figure S19. % imine formation with time from the condensation reaction of dimethyl-5-NH_2-bdc ligand and following aldehydes, 2-formylpyridine, 3-formylpyridine, 4-formylpyridine and benzaldehyde.

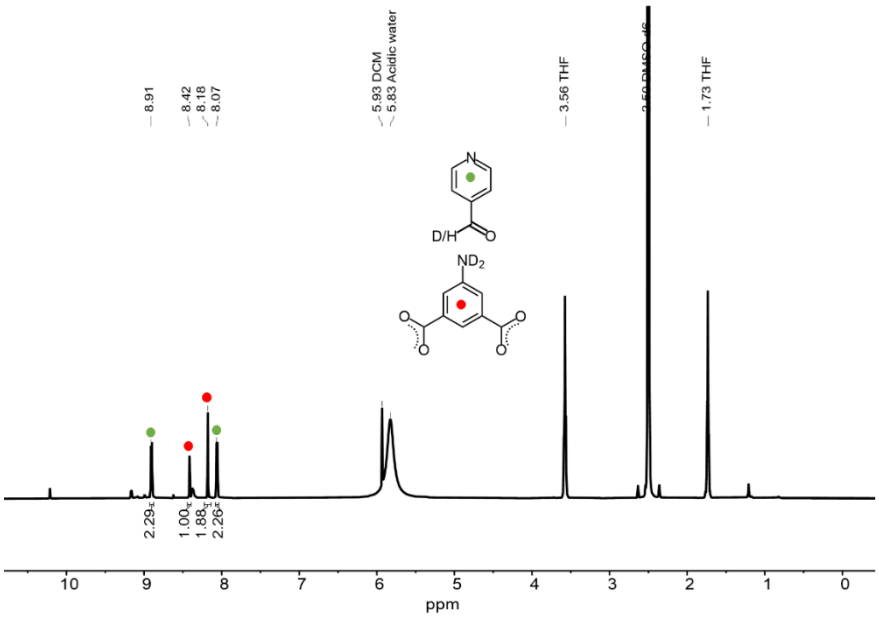

Figure S20. ^{1}H-NMR spectrum of DCl digested Mo_{24}(4-pyridineimine-bdc)$_{24}$ in DMSO-d_6. Hydrolysis of the imine under these conditions affords aldehyde where the aldehyde-proton is partially exchanged with deuterated solvent. The ratio of aldehyde to amine in hydrolyzed sample (~1:1) in conjunction with IR spectra of the imine-based material suggests stoichiometric imine in the starting material.

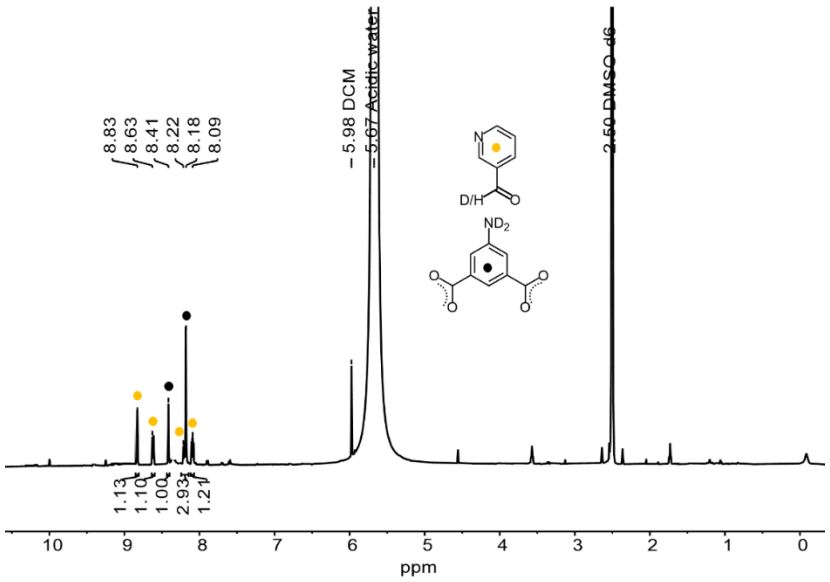

Figure S21. ^{1}H-NMR spectrum of DCl digested Mo_{24}(3-pyridineimine-bdc)$_{24}$ in DMSO-d_6. Hydrolysis of the imine under these conditions affords aldehyde where the aldehyde-proton is partially exchanged with deuterated solvent. The ratio of aldehyde to amine in hydrolyzed sample (~1:1) in conjunction with IR spectra of the imine-based material suggests stoichiometric imine in the starting material.

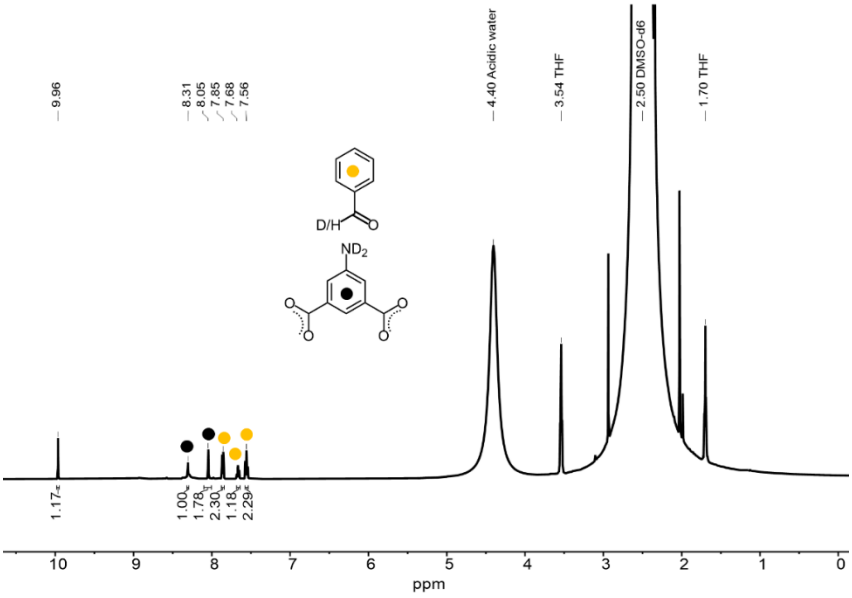

Figure S22. ^{1}H-NMR spectrum of DCl digested Mo_{24}(benzalimine-bdc)$_{24}$ in DMSO-d_6. Hydrolysis of the imine under these conditions affords aldehyde where the aldehyde-proton is partially exchanged with deuterated solvent. The ratio of aldehyde to amine in hydrolyzed sample (~1:1) in conjunction with IR spectra of the imine-based material suggests stoichiometric imine in the starting material.

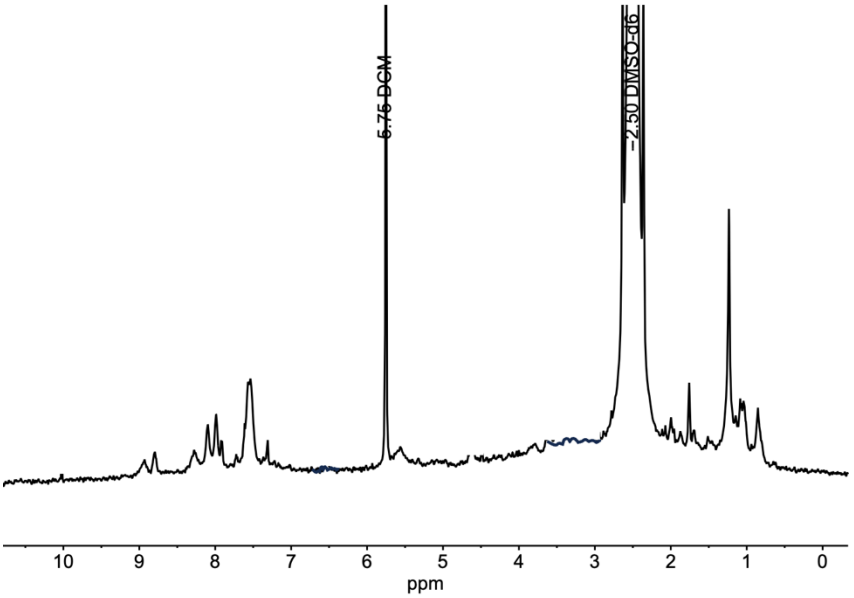

Figure S22(a). ^{1}H-NMR spectrum of Mo_{24}(benzalimine-bdc)$_{24}$ in DMSO-d_6. Non digested NMR are diffused and doesn't allow quantification.

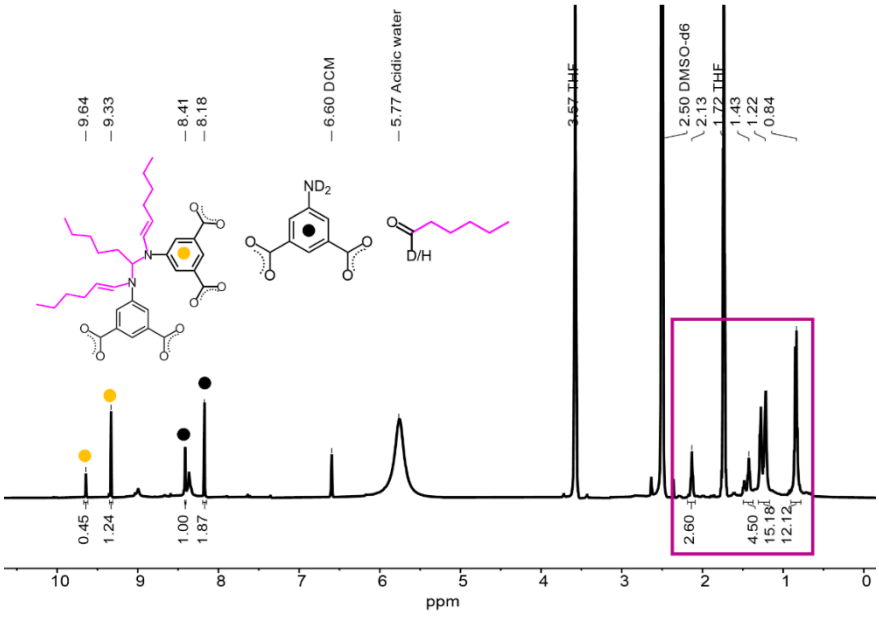

Figure S23. ^{1}H-NMR spectrum of DCl digested Mo_{24}(hex-imine-bdc)$_{24}$ in DMSO-d_6. Hydrolysis of the imine under these conditions affords aldehyde where the aldehyde-proton is partially exchanged with deuterated solvent. The ratio of aldehyde to amine in hydrolyzed sample (~1:1) in conjunction with IR spectra of the imine-based material suggests stoichiometric imine in the starting material.

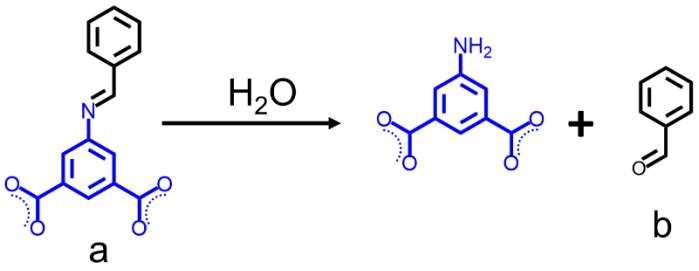

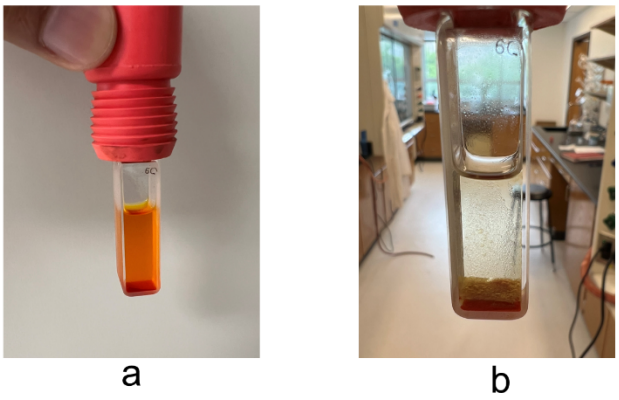

Figure S24. (a) Solubility of Mo_{24}(benzalimine-bdc)$_{24}$ in THF and (b) losing solubility upon hydrolysis of imine bond.

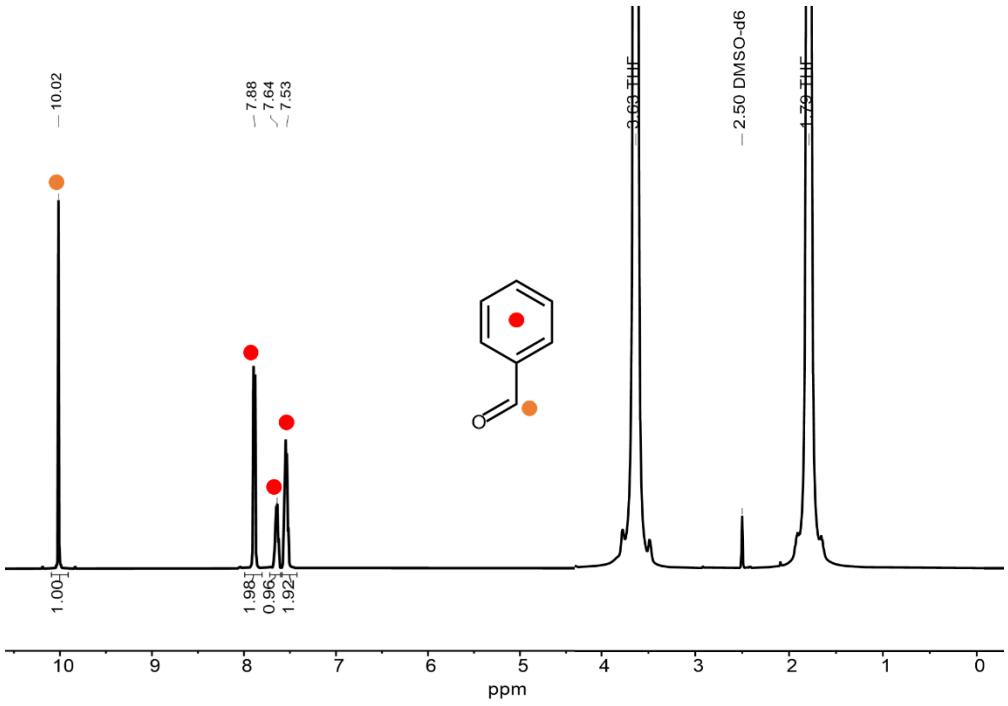

Figure S25. ^{1}H-NMR spectrum of free benzaldehyde from the reaction scheme of Figure S24.

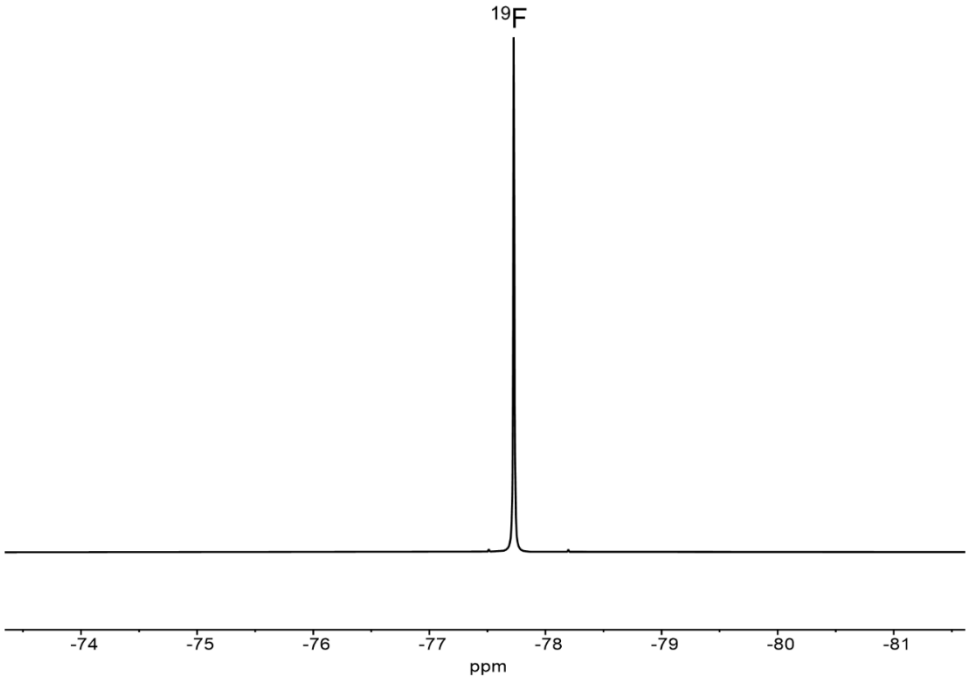

Figure S26. ^{19}F-NMR spectrum of Pd(OTf)$_2$_Mo$_{24}$(2-pyridineimine-bdc)$_{24}$ in DMSO-d$_6$.

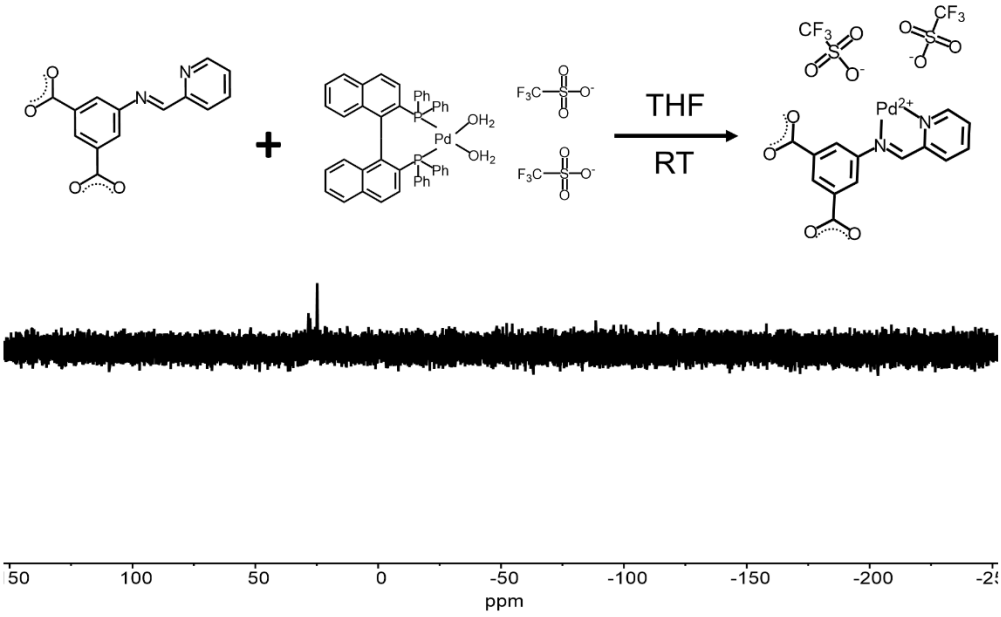

Figure S27. ^{31}P-NMR spectrum of Pd(OTf)$_2$_Mo$_{24}$(2-pyridineimine-bdc)$_{24}$ in DMSO-d$_6$.

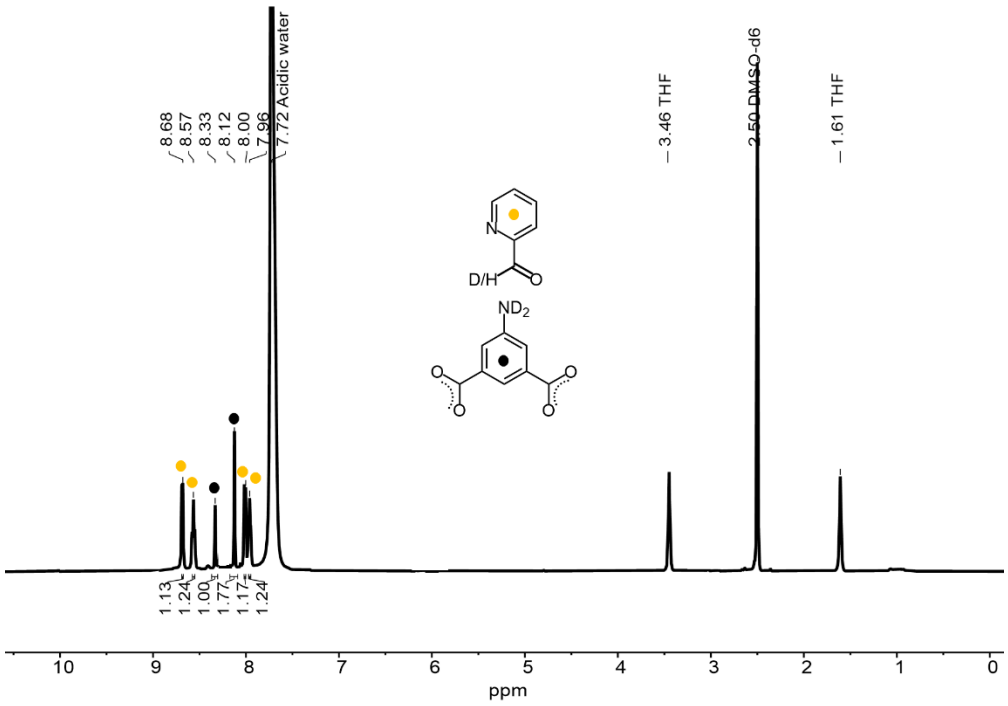

Figure S28. ^{1}H-NMR spectrum of DCl digested $Pd(OTf)_2$_Mo_{24}(2-pyridineimine-bdc)$_{24}$ in DMSO-d_6.

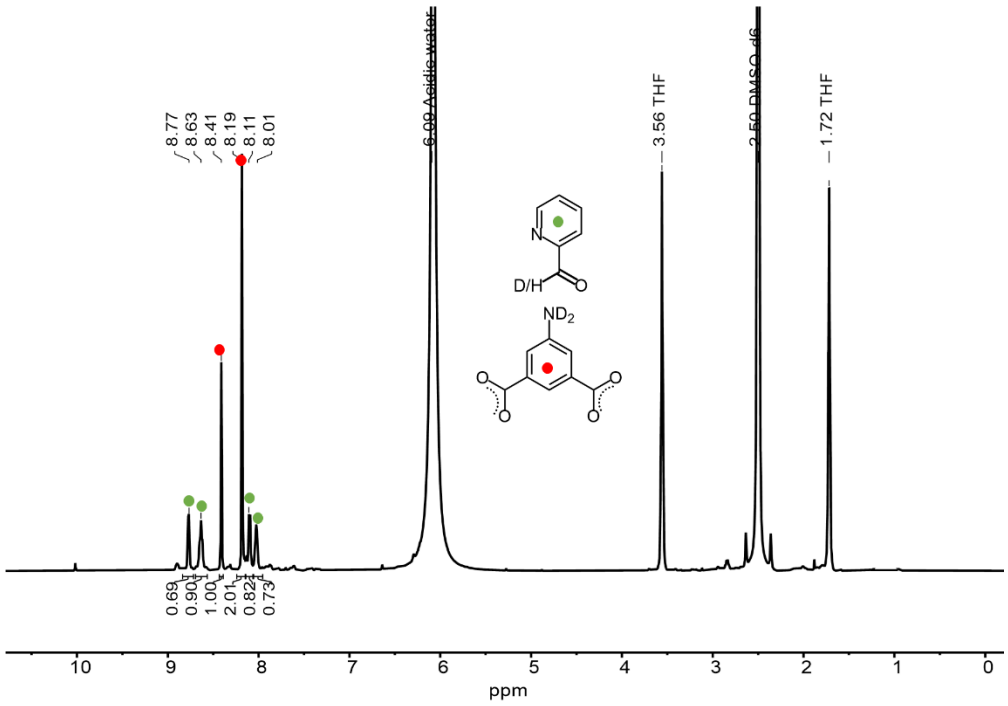

Figure S29. ^{1}H-NMR spectrum of DCl digested $CoCl_2$_Mo_{24}(2-pyridineimine-bdc)$_{24}$ in DMSO-d_6.

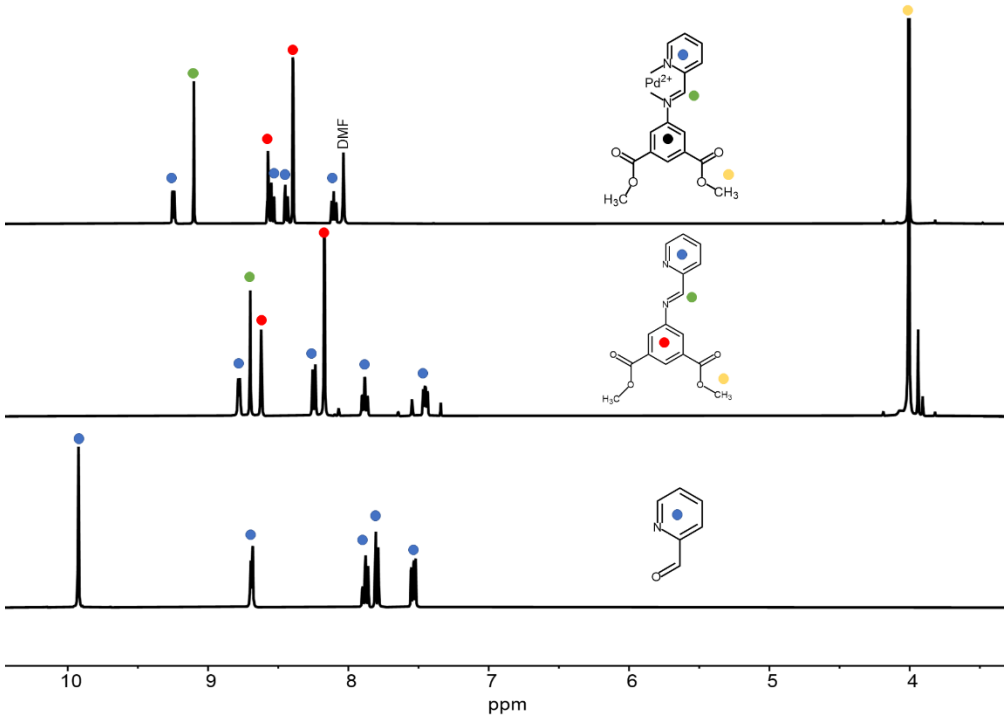

Figure S30. ^{1}H-NMR spectra of 2-formylpyridine, bottom; dimethyl-2-pyridineimine-bdc, middle; and Pd(OTf)$_2$_dimethyl-2-pyridineimine-bdc, top.

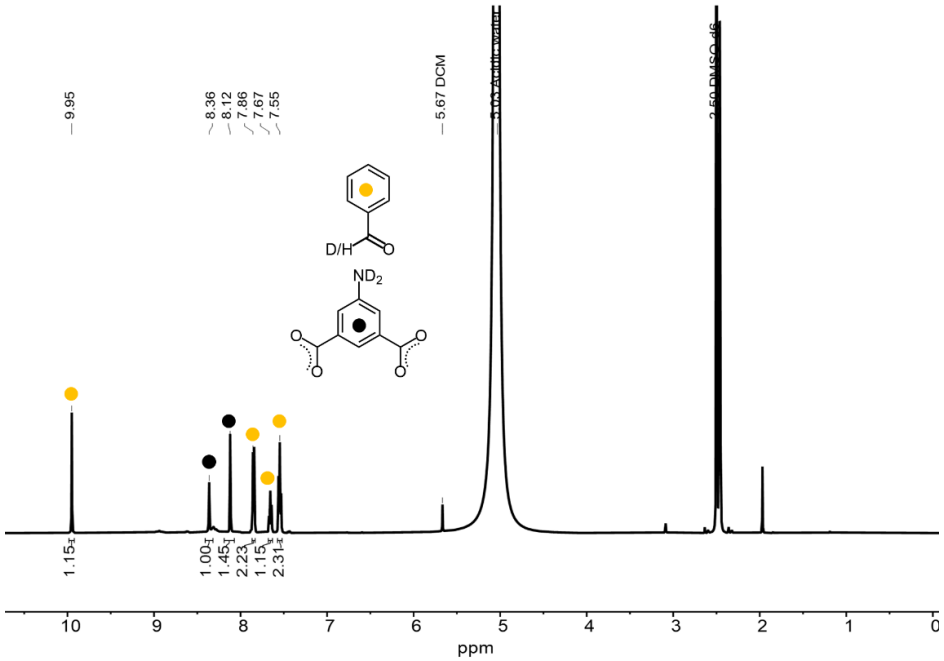

Figure S30(a). ^{1}H-NMR spectrum of DCl digested Mo_{24}(benzalimine-bdc)$_{24}$ in DMSO-d$_6$ where Mo_{24}(5-NH$_2$-bdc)$_{24}$ cage dissolved in DMSO was functionalized with benzaldehyde.

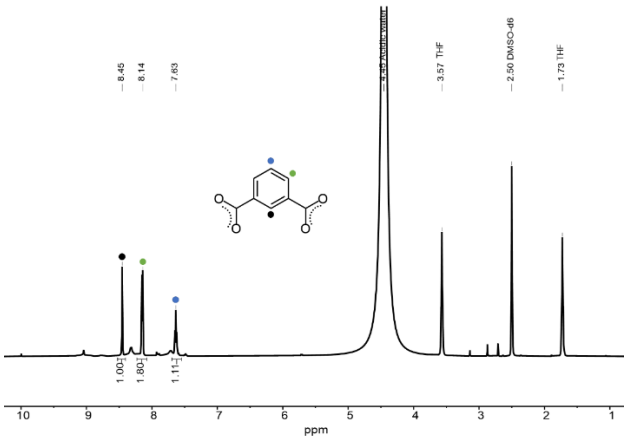

Figure S30(b). ^{1}H-NMR spectrum of DCl digested Mo_{24}(m-bdc)$_{24}$ in DMSO-d_6 reacted with 2-pyridinealdehyde.

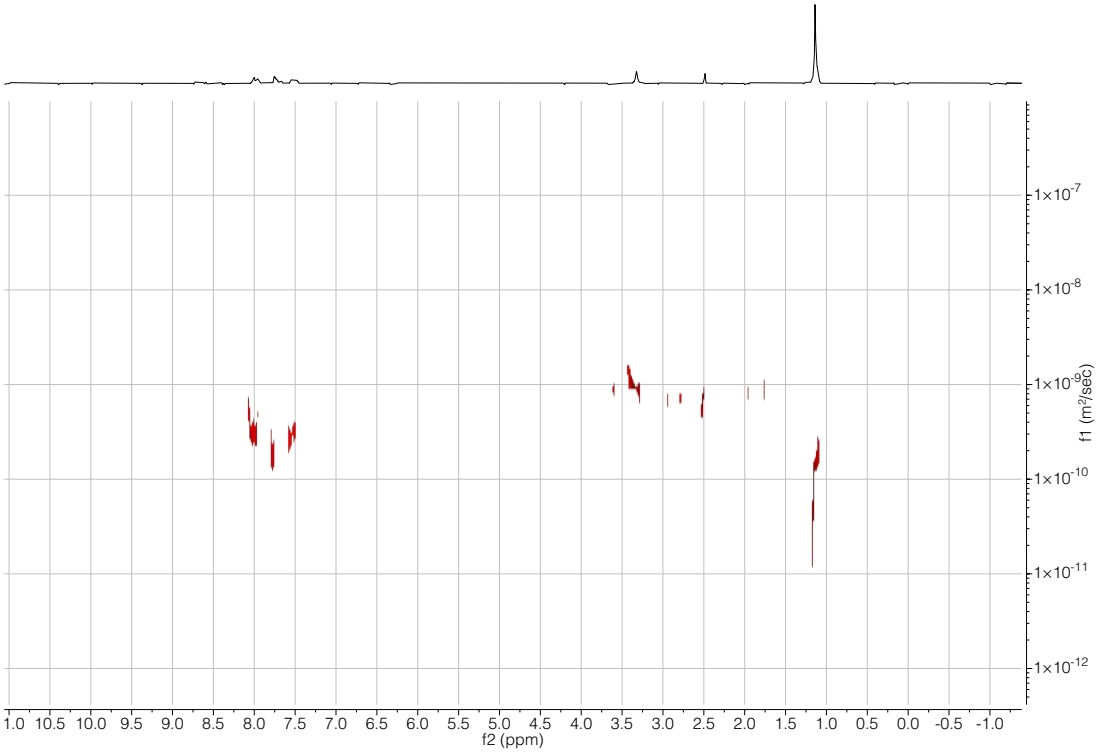

Figure S30(c). DOSY NMR of [(Mg$_4$SC4A)$_4$(μ$_4$-OH)$_4$(2-pyridineimine-bdc)$_8$] in DMSO-d_6. The peaks at ~1x10^{-10} m^2/sec correspond to cage while those at ~1x10^{-9} m^2/sec are solvent.[7]

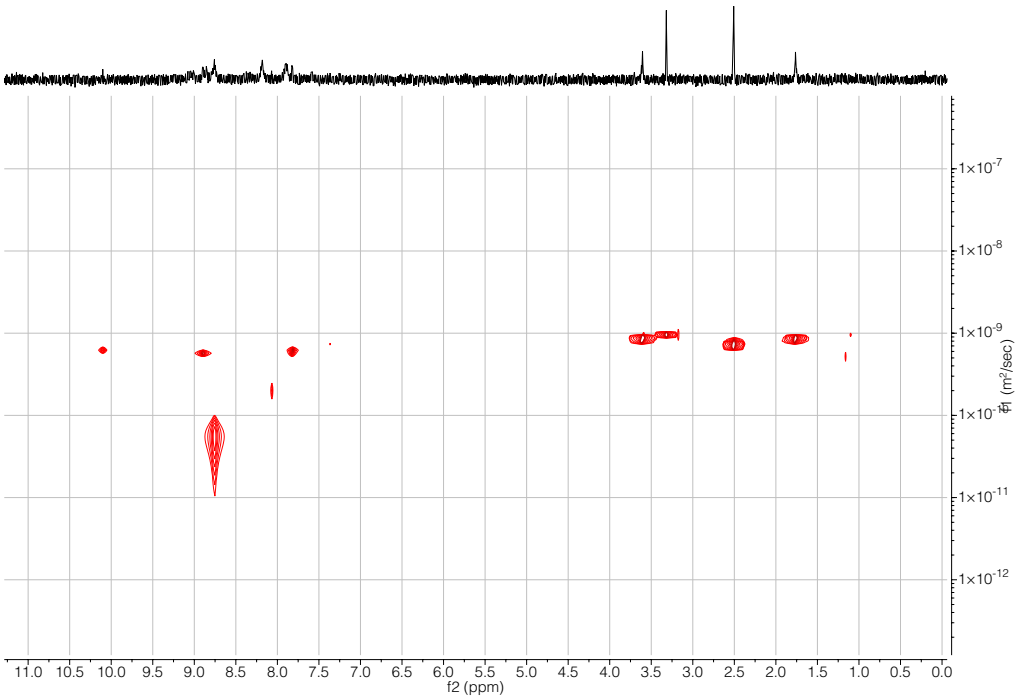

Figure S30(d). DOSY NMR of Mo_{24}(2-pyridineimine-bdc)$_{24}$ in DMSO-d_6. The peaks at ~1x10^{-10} m^2/sec correspond to cage while those at ~1x10^{-9} m^2/sec are solvent and excess aldehyde reagent. The paragmagnetism of the cage makes resolution of all peaks difficult.[7]

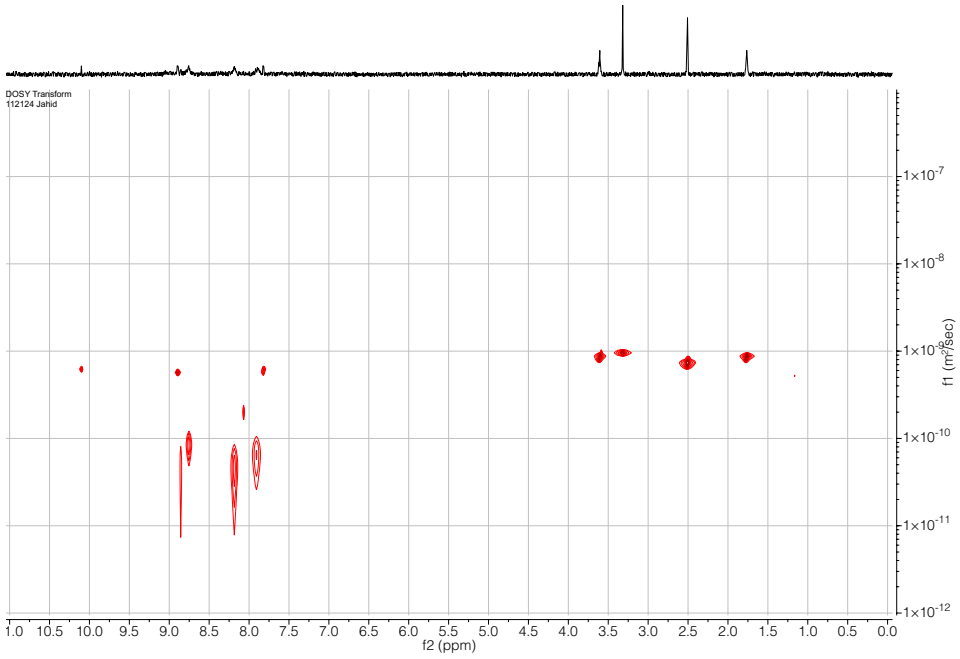

Figure S30(e). DOSY NMR of Mo_{24}(3-pyridineimine-bdc)$_{24}$ in DMSO-d_6. The peaks at ~1x10^{-10} m^2/sec correspond to cage while those at ~1x10^{-9} m^2/sec are solvent and excess

aldehyde reagent. The paragmagnetism of the cage makes resolution of all peaks difficult.[7]

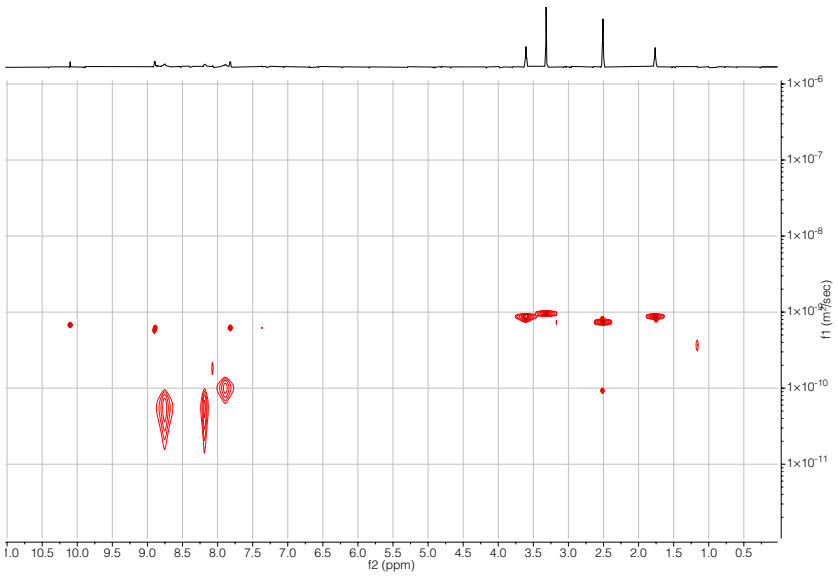

Figure S30(f). DOSY NMR of Mo_{24}(4-pyridineimine-bdc)$_{24}$ in DMSO-d^6. The peaks at ~1x10^{-10} m^2/sec correspond to cage while those at ~1x10^{-9} m^2/sec are solvent and excess aldehyde reagent. The paragmagnetism of the cage makes resolution of all peaks difficult.[7]

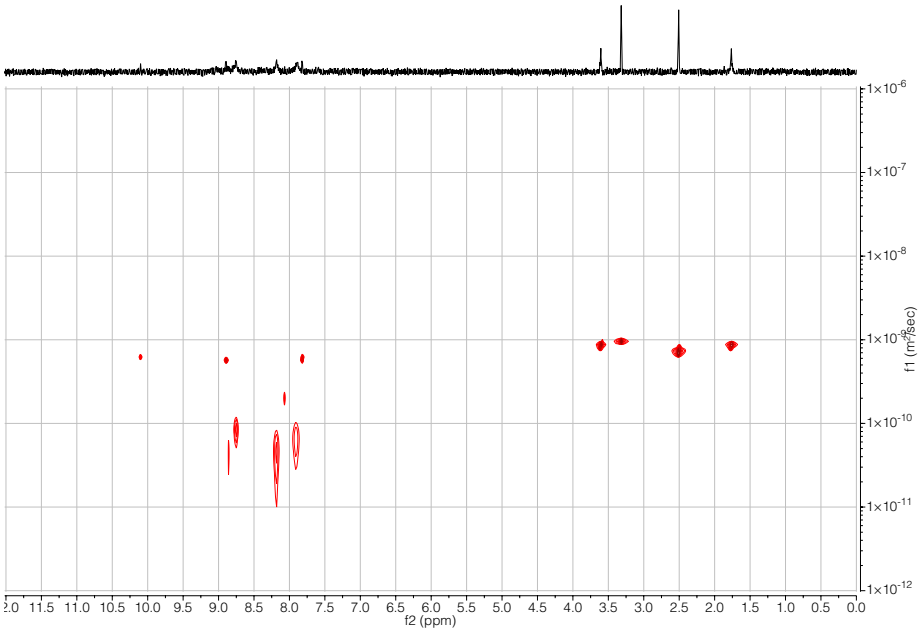

Figure S30(g). DOSY NMR of Mo_{24}(benzalimine-bdc)$_{24}$ in DMSO-d_6. The peaks at ~1x10^{-10} m^2/sec correspond to cage while those at ~1x10^{-9} m^2/sec are solvent and excess aldehyde reagent. The paragmagnetism of the cage makes resolution of all peaks difficult.[7]

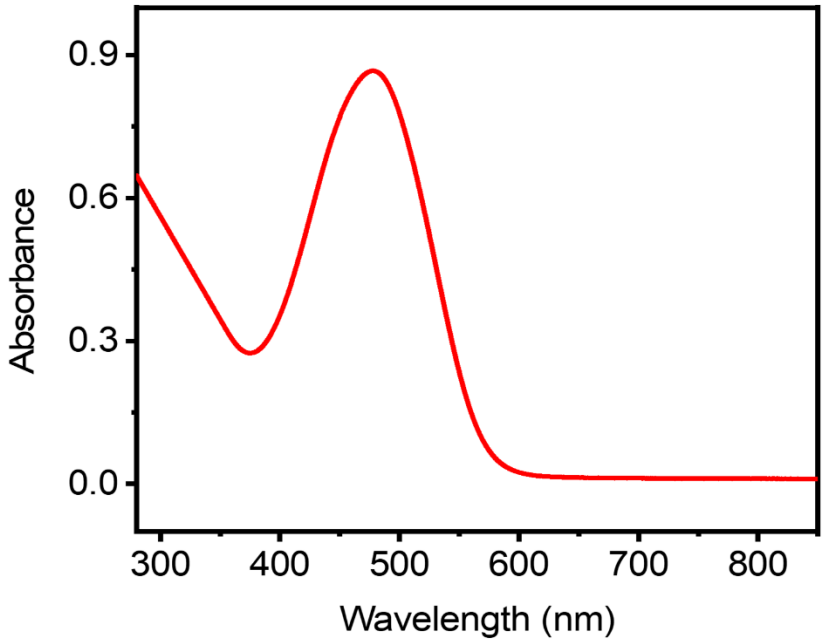

Figure S31. UV-vis absorption of Mo_{24}(3-pyridineimine-bdc)$_{24}$ in DMSO.

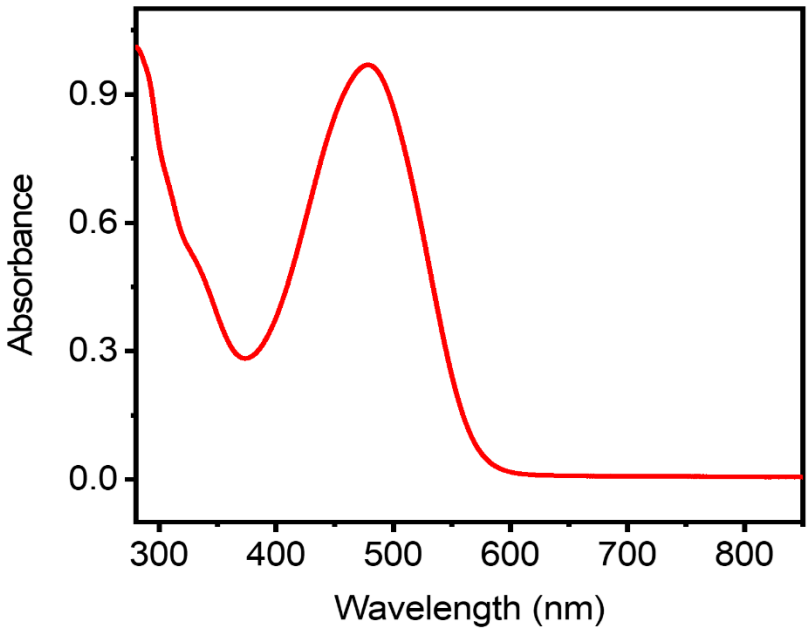

Figure S32. UV-vis absorption of Mo_{24}(4-pyridineimine-bdc)$_{24}$ in DMSO.

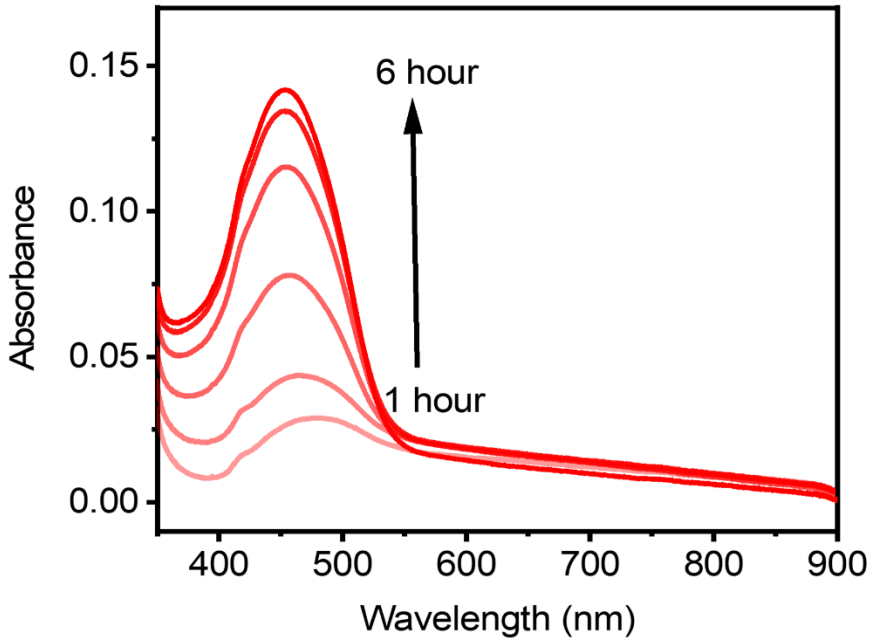

Figure S33. Increased absorbance of Mo_{24}(hex-imine-bdc)$_{24}$ in THF due to attaining solvent processability upon hexanal functionalization.

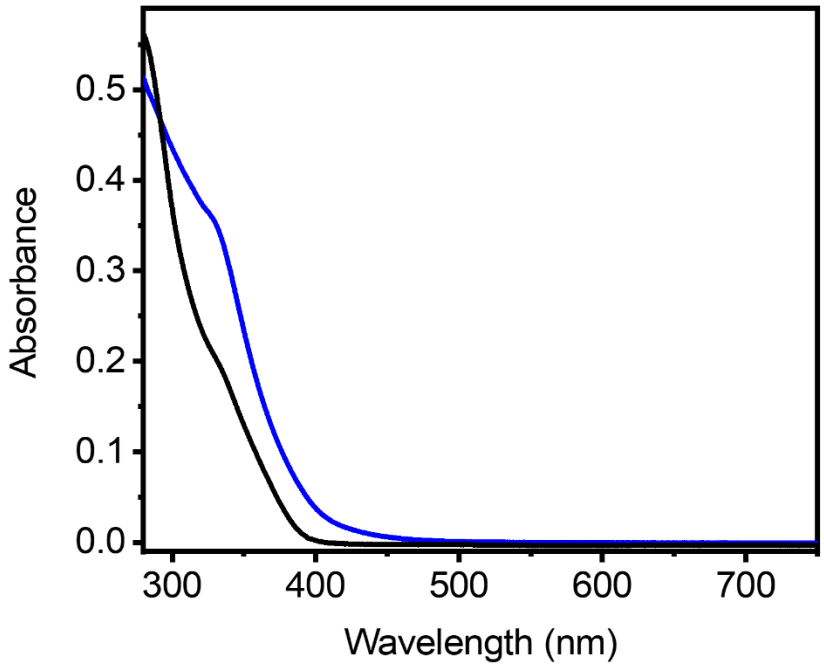

Figure S34. UV-vis absorption of dimethyl-2-pyridineimine-bdc metallated with $PdCl_2$, black, and $Pd(OTf)_2$, blue.

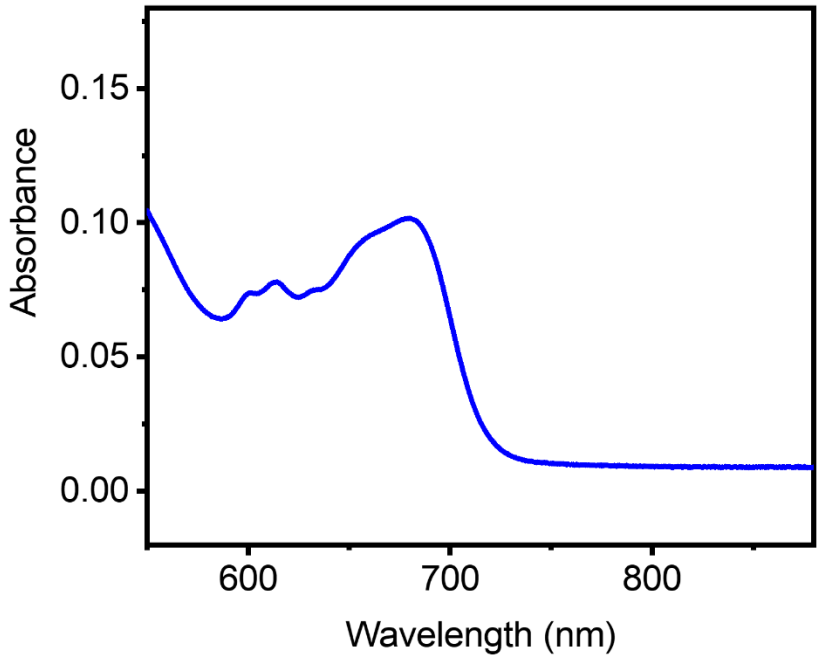

Figure S35. UV-vis absorption of $CoCl_2$_dimethyl-2-pyridineimine-bdc in DMSO.

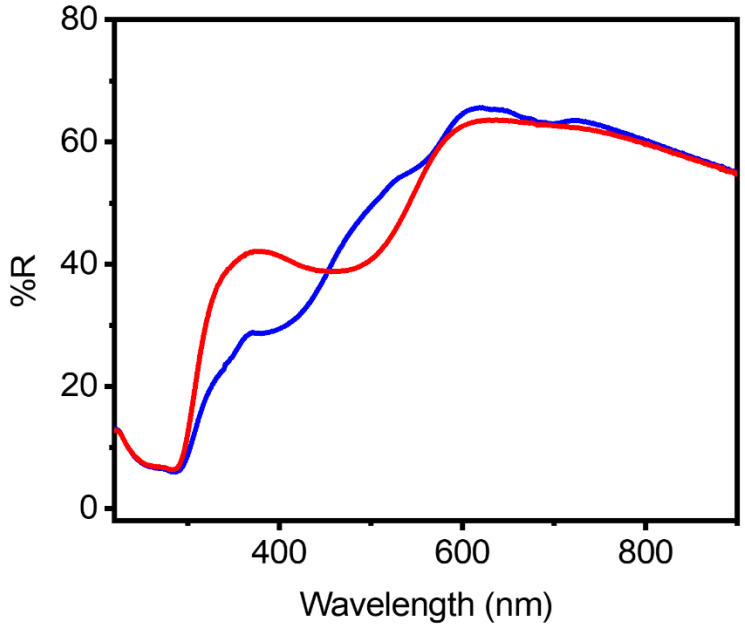

Figure S36. Diffuse reflectance of $CoCl_2$_Mo_{24}(2-pyridineimine-bdc)$_{24}$, red; and $CoCl_2$_dimethyl-2-pyridineimine-bdc, blue.

Absorption study: $CoCl_2$ metallation

THF solution of 0.01 mmol $CoCl_2$ was prepared in a cuveet and initial absorbance was recorded. Equivalent amount of Mo_{24}(2-pyridineimine-bdc)$_{24}$ was added to the solution and absorbance of the THF solution was measured in every 2 hours.

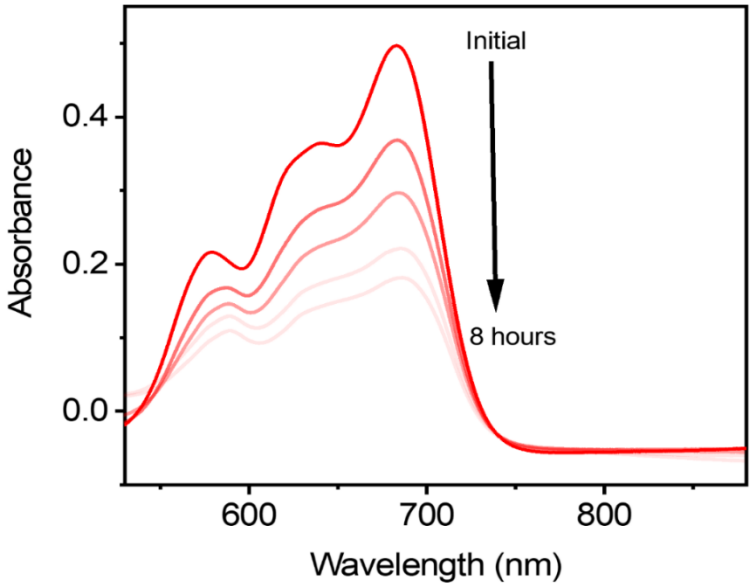

Figure S37. Decreased absorbance of $CoCl_2$ in THF due to losing $CoCl_2$ while the formation of $CoCl_2$_Mo_{24}(2-pyridineimine-bdc)$_{24}$.

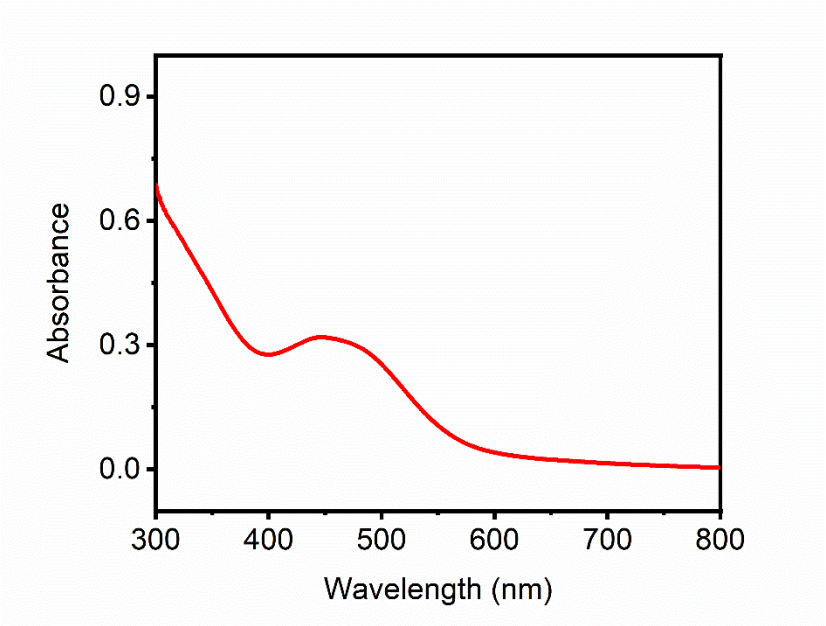

Figure S38. UV-vis absorption of Mo_{24}(2-pyridineimine-bdc)$_{24}$ in DMSO.

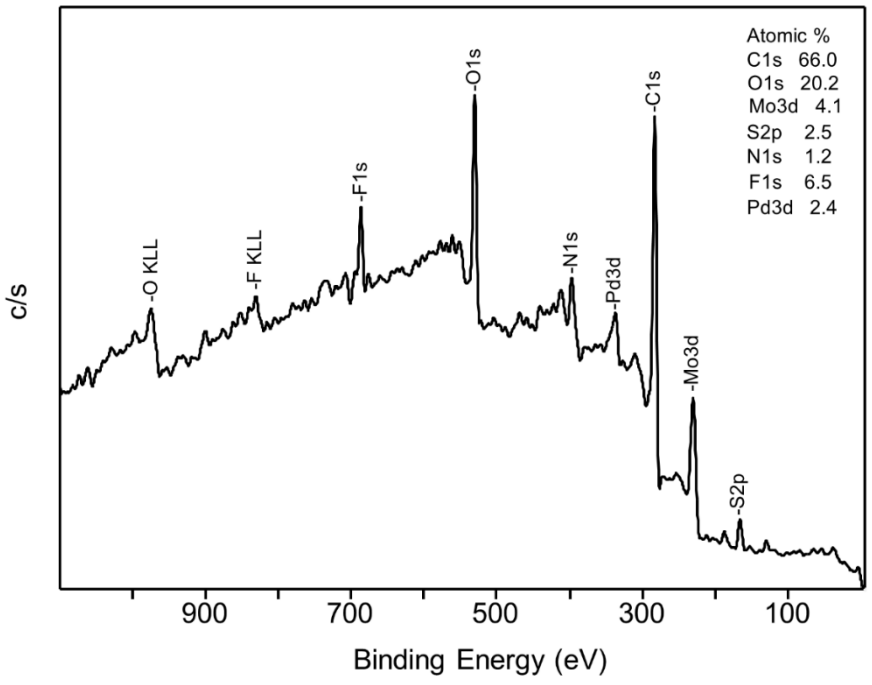

Figure S39. X-ray photoelectron spectroscopy of $Pd(OTf)_2$_Mo_{24}(2-pyridineimine-bdc)$_{24}$.

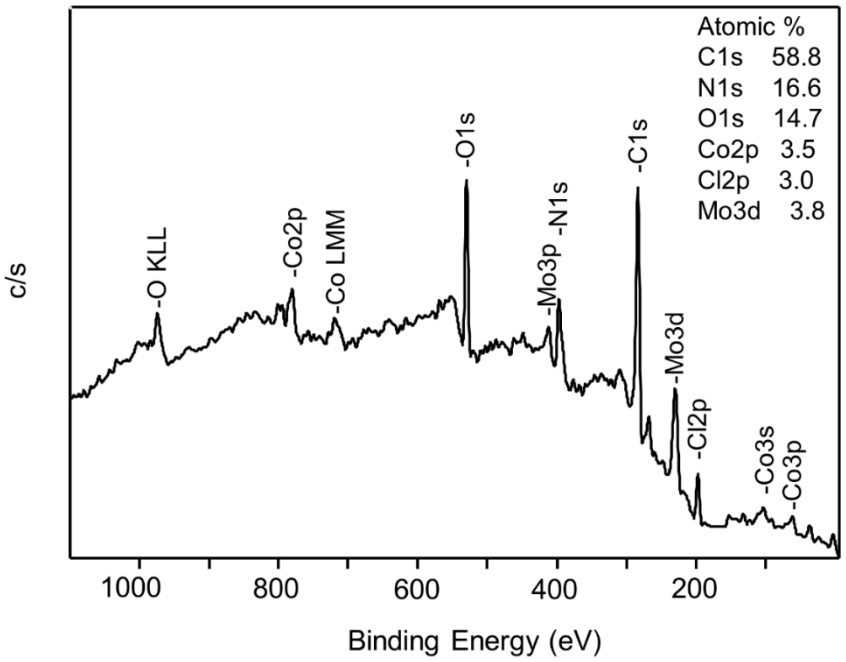

Figure S40. X-ray photoelectron spectroscopy of $CoCl_2$_Mo_{24}(2-pyridineimine-bdc)$_{24}$.

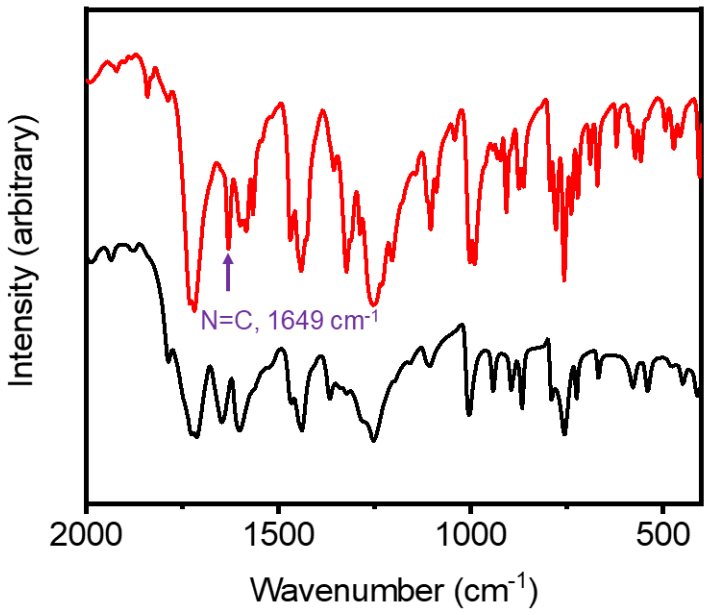

Figure S41(a). IR spectra of dimethyl-5-NH_2-bdc, black; dimethyl-2-pyridineimine-bdc, red.

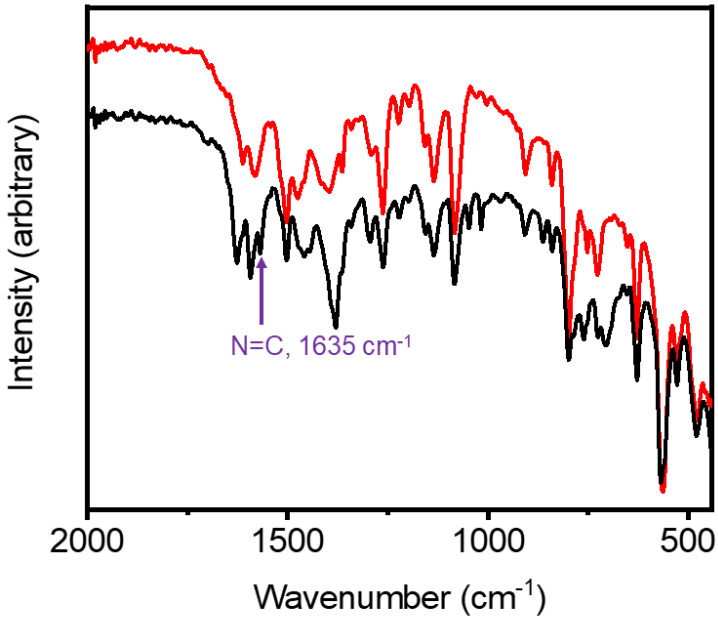

Figure S41(b). IR spectra of $[(Mg_4SC4A)_4(\mu_4\text{-}OH)_4(5\text{-}NH_2\text{-}bdc)_8]^{4-}$, red; $[(Mg_4SC4A)_4(\mu_4\text{-}OH)_4(2\text{-}pyridineimine\text{-}bdc)_8]$, black.

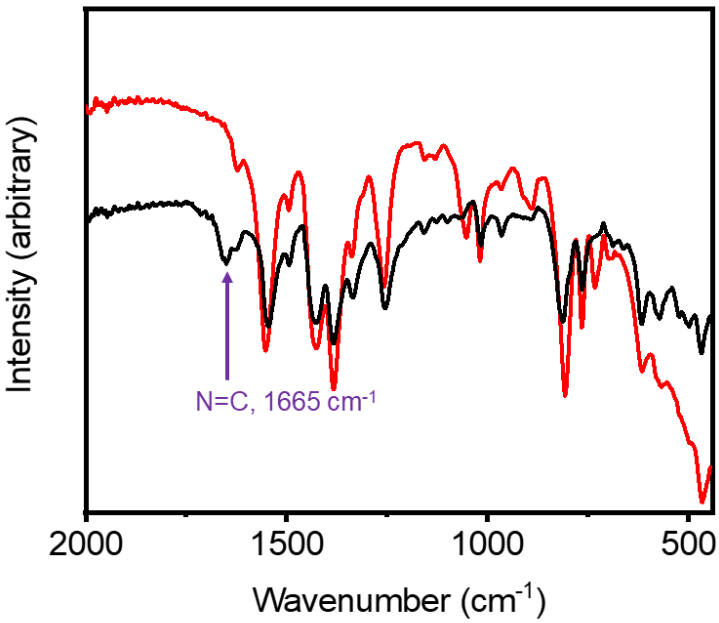

Figure S41(c). IR spectra of $Zr_{12}(\mu_3\text{-}O)_4(\mu_2\text{-}OH)_{12}(Cp)_{12}(2\text{-}NH_2\text{-}bdc)_6]Cl_4$, red; $Zr_{12}(\mu_3\text{-}O)_4(\mu_2\text{-}OH)_{12}(Cp)_{12}(2\text{-}pyridineimine\text{-}bdc)_6]Cl_4$, black.

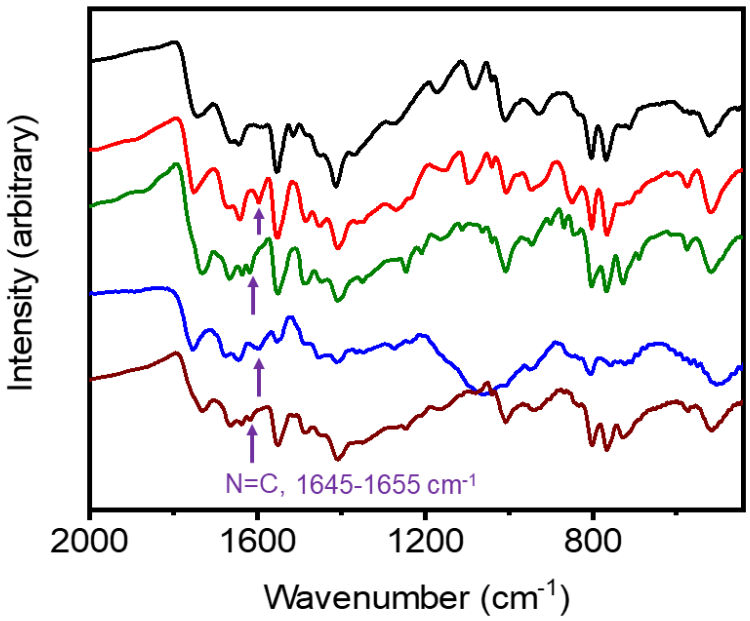

Figure S41(d). IR spectra of Mo_{24}(5-NH_2-bdc)$_{24}$, black; Mo_{24}(2-pyridineimine-bdc)$_{24}$, red; Mo_{24}(3-pyridineimine-bdc)$_{24}$, olive; Mo_{24}(4-pyridineimine-bdc)$_{24}$, blue; and Mo_{24}(benzalimine-bdc)$_{24}$, red wine.

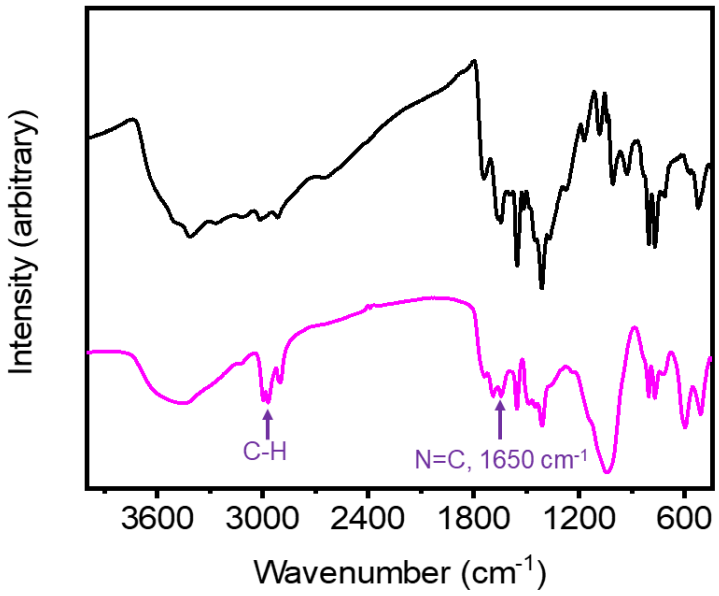

Figure S41(e). IR spectra of Mo_{24}(5-NH_2-bdc)$_{24}$, black; Mo_{24}(hex-imine-bdc)$_{24}$, pink.

Figure S42. Benzene solubility of Mo_{24}(benzalimine-bdc)$_{24}$.

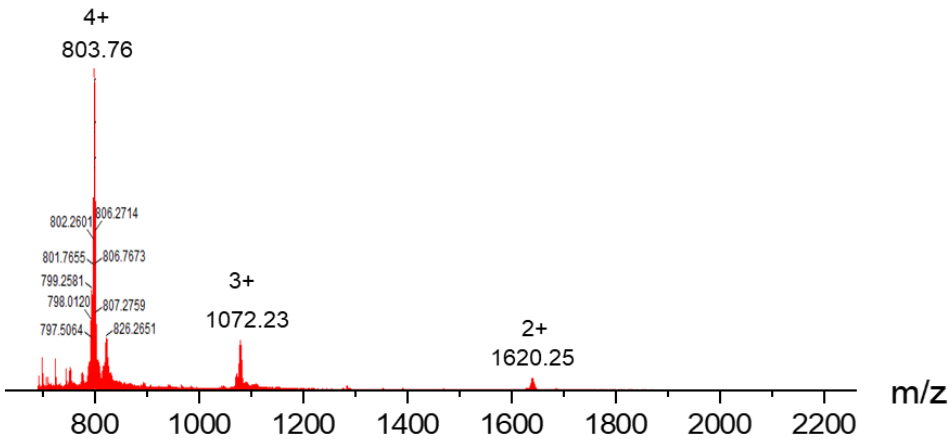

Figure S43. LC-MS spectra of MeOH dissolved $Zr_{12}(\mu_3\text{-}O)_4(\mu_2\text{-}OH)_{12}(Cp)_{12}(2\text{-}NH_2\text{-}bdc)_6]Cl_4$ where the peak at 803.76 m/z corresponds to the cationic $Zr_{12}(\mu_3\text{-}O)_4(\mu_2\text{-}OH)_{12}(Cp)_{12}(2\text{-}NH_2\text{-}bdc)_6]^{4+}$ for a molecular mass of ~3215 amu. Peaks at 1072.23 m/z and 1620.25 m/z indicate the cationic cage of 3+ and 2+ due to ionization from μ_2-OH.

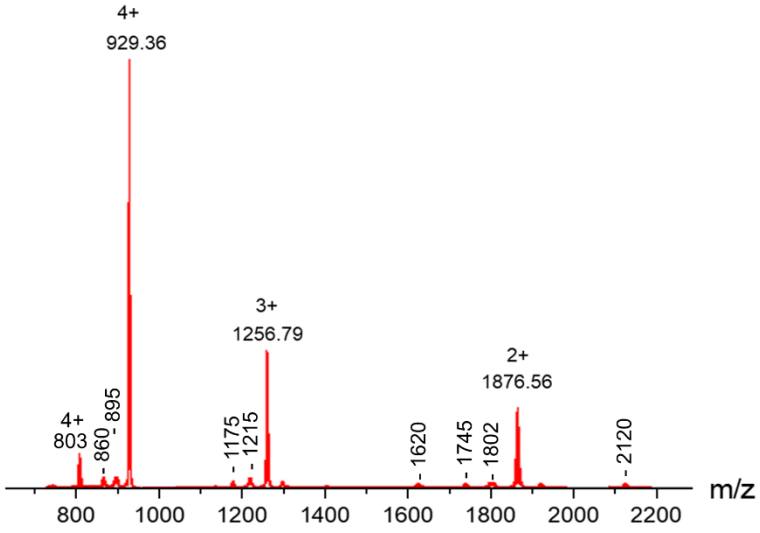

Figure S44. The LC-MS spectra of MeOH-dissolved $Zr_{12}(\mu_3\text{-}O)_4(\mu_2\text{-}OH)_{12}(Cp)_{12}$(2-pyridineimine-bdc)$_6]Cl_4$ show a peak at 929.36 m/z, which corresponds to the cationic $Zr_{12}(\mu_3\text{-}O)_4(\mu_2\text{-}OH)_{12}(Cp)_{12}$(2-pyridineimine-bdc)$_6]^{4+}$, with a molecular mass of approximately 3717 amu. This is about 502 amu greater than the molecular mass of $Zr_{12}(\mu_3\text{-}O)_4(\mu_2\text{-}OH)_{12}(Cp)_{12}$(2-$NH_2$-bdc)$_6]^{4+}$, due to the incorporation of six pyridineimine groups replacing the six -NH2 groups. Peaks at 1256 m/z and 1876 m/z indicate the presence of cationic species with 3+ and 2+ charges, resulting from the ionization of $Zr_{12}(\mu_3\text{-}O)_4(\mu_2\text{-}OH)_{12}(Cp)_{12}$(2-pyridineimine-bdc)$_6]^{4+}$ through the ionization from μ_2-OH.

Data collection for $CoCl_2$_dimethyl-2-pyridineimine-bdc

The data collection was carried out using Mo Kα radiation (graphite monochromator) with a frame time of 2, 5, and 30 seconds and a detector distance of 4.0 cm. A collection strategy was calculated and complete data to a resolution of 0.81 Å with a redundancy of 9.46 were collected. Nine major sections of frames were collected with 1.00º ϕ and ω scans. A total of 2116 frames were collected. The total exposure time was 9.24 hours. The frames were integrated with the Bruker SAINT software package[1] using a narrow-frame algorithm. The integration of the data using a monoclinic unit cell yielded a total of 35180 reflections to a maximum θ angle of 26.02° (0.81 Å resolution), of which 3624 were independent (average redundancy 9.708, completeness = 99.9%, Rint = 6.23%, Rsig = 3.17%) and 3330 (91.89%) were greater than $2\sigma(F^2)$. The final cell constants of a = 23.3352(6) Å, b = 11.9100(3) Å, c = 16.3910(7) Å, β = 126.0298(6)°, volume = 3684.0(2) Å3 , are based upon the refinement of the XYZ-centroids of 9813 reflections above 20

σ(I) with 5.019° < 2θ < 52.73°. Data were corrected for absorption effects using the Multi-Scan method (SADABS[2]). The ratio of minimum to maximum apparent transmission was 0.779. The calculated minimum and maximum transmission coefficients (based on crystal size) are 0.9140 and 0.9550.

Structure solution and refinement

The space group C2/c was determined based on intensity statistics and systematic absences. The structure was solved with intrinsic-methods and refined with full-matrix-least squares using the SHELX suite of programs in the Olex2.[3,4,5] All non-hydrogen atoms were refined with anisotropic displacement parameters. The hydrogen atoms were placed in ideal positions and refined as riding atoms with relative isotropic displacement parameters. The final anisotropic full-matrix least-squares refinement on F^2 with 243 variables converged at R1 = 3.08%, for the observed data and wR2 = 8.61% for all data. The goodness-of-fit was 1.075. The largest peak in the final difference electron density synthesis was 0.265 e- /Å^3 and the largest hole was -0.438 e- /Å^3 with an RMS deviation of 0.057 e- /Å^3. On the basis of the final model, the calculated density was 1.458 g/cm3 and F(000), 1668 e-.

Data collection for $PdCl_2$_dimethyl-2-pyridineimine-bdc

X-ray structural analysis: A crystal was mounted using viscous oil onto a plastic mesh and cooled to the data collection temperature. Data were collected on a D8 Venture Photon diffractometer with Cu- Kα radiation (λ = 1.54178 Å) focused with Goebel mirrors. Unit cell parameters were obtained from fast scan data frames, 1º/s ω, of an Ewald hemisphere. The unit-cell dimensions, equivalent reflections and systematic absences in the diffraction data are uniquely consistent with P21/c. The data were treated with multi-scan absorption corrections.[6] Structures were solved using intrinsic phasing methods[3] and refined with full-matrix, least-squares procedures on F^2.[4]

Non-hydrogen atoms were refined with anisotropic displacement parameters. Hydrogen atoms were treated as idealized contributions with geometrically calculated positions and with U_{iso} equal to 1.2 U_{eq} (1.5 U_{eq} for methyl) of the attached atom. Atomic scattering factors are contained in the SHELXTL program library.[7] The structure has been deposited at the Cambridge Structural Database under CCDC 2379514.

Table 1. Crystal data and structure refinement details $PdCl_2$_dimethyl-2-pyridineimine-bdc

Compound	$PdCl_2$_dimethyl-2-pyridineimine-bdc
Sum formula	$C_{16}H_{14}Cl_2N_2O_4Pd$
Moiety formula	$C_{16}H_{14}Cl_2N_2O_4Pd$
Formula weight	475.59

Temperature, K	100
Crystal system	monoclinic
Space group	P21/c
Cell dimension	
a, Å	13.1543(12)
b, Å	8.5115(8)
c, Å	16.4253(15)
α, °	90
β, °	110.595(5)
γ, °	90
Volume, $Å^3$	1721.5(3)
Z	4
ρ_{calc}, g/cm^3	1.835
μ/mm^{-1}	11.778
F(000)	944.0
Reflections collected	17566
Independent reflections	2935 [R_{int} = 0.0637, R_{sigma} = 0.0496]
Data/restraints/parameters	2935/0/228
Goodness-of-fit F^2	1.083
Final R indexes [I>=2σ (I)]	R_1 = 0.0407, wR_2 = 0.0819
Final R indexes [all data]	R_1 = 0.0455, wR_2 = 0.0838
CCDC	2379514

Table 2. Crystal data and structure refinement details of $CoCl_2$_dimethyl-2-pyridineimine-bdc

Compound	$CoCl_2$_dimethyl-2-pyridineimine-bdc
Sum formula	$C_{36}H_{34}Cl_2N_6O_8Co$
Moiety formula	$C_{36}H_{34}Cl_2N_6O_8Co$
Formula weight	808.52
Temperature, K	173(2)
Crystal system	Monoclinic
Space group	C2/c
Cell dimension	
a, Å	23.3352(6)
b, Å	11.91003(3)
c, Å	16.3910(7)
α, °	90

β, °	126.0298(6)
γ, °	90
Volume, $Å^3$	3684.0(2)
Z	4
ρ_{calc}, Mg/m^3	1.458
Absorption coefficient, mm^{-1}	0.671
F(000)	1668
Reflections collected	35180
Independent reflections	3624
Data / restraints / parameters	3624 / 0 /243
Goodness-of-fit on F^2	1.075
Final R indices [I>2σ (I)	R1 = 0.0308, wR2 = 0.0825
R indices (all data)	R1 = 0.0338, wR2 = 0.0861
CCDC	2378545

References

1. SAINT V8.40A (2020), Bruker AXS, Madison, WI.
2. L. Krause, R. Herbst-Irmer, G. M. Sheldrick and D. Stalke, *J. Appl. Cryst.*, 2015, **48**, 3-10.
3. G. M. Sheldrick, *Acta Cryst*. 2015 **A71**, 3-8.
4. G. M. Sheldrick, *Acta Cryst.* 2015, **C71**, 3-8.
5. O. V. Dolomanov, L. J. Bourhis, R. J. Gildea, J. A. K. Howard and H. Puschmann, *J. Appl. Cryst.* 2009, **42**, 339-341.
6. Apex3 [Computer Software]; Bruker AXS Inc.: Madison, WI, USA, 2015.
7. G. A. Taggart, A. Guliyeva, K. Kim, G. P. A. Yap, D. J. Pochan, T. H. Epps, E. D. Bloch, *J. Phys. Chem. C 2023*, **127**, 2379-2386.